CHAPTER 1

Atomlike Building Units of Adjustable Character: Solid-State and Solution Routes to Manipulating Hexanuclear Transition Metal Chalcohalide Clusters

ERIC J. WELCH and JEFFREY R. LONG

Department of Chemistry
University of California, Berkeley
Berkeley, CA 94720

CONTENTS

I. INTRODUCTION 2

A. Cluster Geometries / 2
B. Electronic Structures / 5

II. SOLID-STATE SYNTHESIS 8

A. Dimensional Reduction / 12
1. Standard Salt Incorporation / 12
2. Core Anion Substitution / 13
3. Heterometal Substitution / 18
4. Interstitial Substitution / 21
B. Low-Temperature Routes / 21

III. SOLUTION METHODS 25

A. Cluster Excision / 25
B. Solution-Phase Cluster Assembly / 26

Progress in Inorganic Chemistry, Vol. 54 Edited by Kenneth D. Karlin

C. Ligand Substitution Reactions / 27
1. Core Anion Exchange / 27
2. Terminal Ligand Exchange / 28

IV. ELECTRONIC PROPERTIES 30

A. Electrochemistry / 30
B. Paramagnetism / 32
C. Photochemistry / 32

V. CLUSTERS AS BUILDING UNITS 33

A. Extended Solid Frameworks / 33
B. Supramolecular Assemblies / 36

VI. CONCLUDING REMARKS 38

ACKNOWLEDGMENTS 38

ABBREVIATIONS 38

REFERENCES 39

1. INTRODUCTION

Over the past two decades, considerable progress has been made in the synthesis and characterization of compounds containing discrete hexanuclear clusters (1–12). Most recently, soluble, molecular forms of these clusters have begun to see use as building units in the construction of extended solid frameworks and supramolecular assemblies. In our view, certain hexanuclear cluster cores are very much akin to a new transition metal ion, but one with a large radius, a fixed coordination geometry, and electronic properties that can be adjusted through synthesis. In particular, clusters of this type are encountered with second- and third-row transition elements of groups 4–7 in reduced oxidation states, accompanied by core halide and/or chalcogenide ligands. Herein, we review the methods available for manipulating the composition of such species, and give a brief overview of their use in solution assembly reactions.

A. Cluster Geometries

The clusters of interest here bear one of three distinct geometries, all of which are based upon a central M_6 unit exhibiting some degree of metal–metal bonding. In two of the geometries, the metal atoms are arranged in an octahedron, while in the third they from a regular trigonal prism. Importantly,

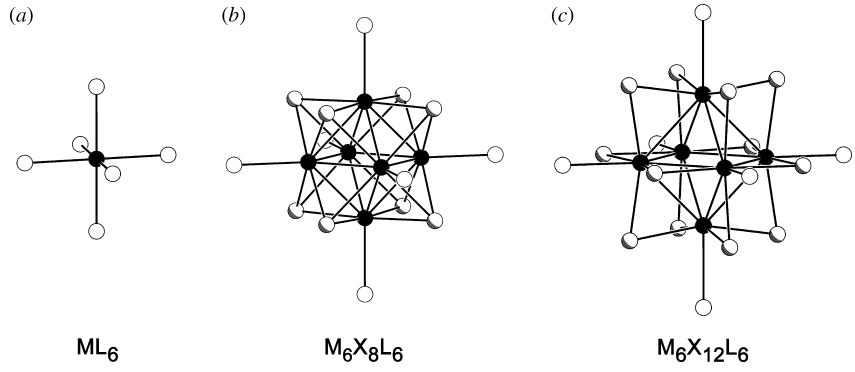

Figure 1. Idealized structures of an octahedral ML_6 complex (*a*), a face-capped octahedral $M_6X_8L_6$ cluster (*b*), and an edge-bridged octahedral $M_6X_{12}L_6$ cluster (*c*). Black, shaded, and white spheres represent metal atoms M, inner-ligands X, and terminal-ligands L, respectively. Each structure conforms to O_h symmetry.

each metal center bears one radially extending terminal ligand L, such that, overall, the outer coordination sphere is analogous to that of an octahedral or trigonal-prismatic metal complex.

For the metals of Groups 6 and 7, the $M_6X_8L_6$ geometry displayed in the middle of Fig. 1 is predominant. Here, the cluster core consists of a perfect octahedron of metal atoms with each face capped by a halide or chalcogenide anion X. The eight core anions form a cube, with the metal atoms positioned approximately within the plane and near the center of each cube face. Thus, each metal center has local C_{4v} symmetry, with a ligand set comprised of an axial ligand L, a square of four equatorial X anions, and a lower, staggered square of four metal atoms. Typical mean M—M bond distances range from 2.601(4) Å in $[Re_6S_8Cl_6]^{4-}$ (13) to 2.681(3) Å in $[Re_6Te_8(CN)_6]^{4-}$ (14), while mean M-X distances range from 2.403(9) Å in $[Re_6S_8Cl_6]^{4-}$ to 2.792(7) Å in $[W_6I_{14}]^{2-}$ (15). Based upon comparisons with analogous ML_6 complexes, the clusters exhibit a core radius of $\sim$2.8 Å, which of course is much larger than the radius of any single transition metal ion. The M_6X_8 core geometry is perhaps most notably observed in the Chevrel phases of the type $A_xMo_6X_8$ (X = S, Se), which have long been of interest for their superconducting and magnetic properties (16–19). This geometry generally does not appear to support the presence of an interstitial atom at the center of the octahedron, with an exception arising in the electron-deficient clusters of Nb_6HI_{11} (20, 21).

Clusters containing metals from groups 4 and 5 show a strong preference for structures based upon the $M_6X_{12}L_6$ geometry shown in Figure 1(*c*). In this case, the core consists of an octahedron of metal atoms with each edge bridged by a halide or chalcogenide anion X. The 12 core anions form a regular cuboctahedron, with the metal atoms positioned near the center but slightly below the plane

of each square face. Accordingly, each metal center has local C_{4v} symmetry, with a ligand set comprised of an axial ligand L, a square of four equatorial X anions, and a lower, eclipsed square of four metal atoms. Typical mean M—M bond distances range from 2.803 Å in Nb_6F_{15} (22) to 3.018(2) Å in $[Nb_6Cl_{18}]^{2-}$ (23), while mean M—X distances range from 2.049 Å in Nb_6F_{15} to 2.797(5) Å in Ta_6I_{14} (24). Note that these clusters tend to be slightly larger than face-capped octahedral clusters, with a core radius of ~3.2 Å, based upon comparisons with analogous ML_6 complexes. The edge-bridged octahedral geometry has also been observed for a single binary group 6 halide: W_6Cl_{18} (25, 26). Importantly, for group 4 metals, this geometry typically occurs with an interstitial main group or transition metal atom situated at the center of the octahedron, giving rise to clusters of generic formula $M_6ZX_{12}L_6$. Clusters of this type are also apparent in numerous reduced rare earth halide phases, although generally only within the confines of a highly condensed framework (1, 5, 6, 10, 27). These interesting rare earth clusters will not be further discussed here, since methods for bringing them into solution have not yet been developed.

An alternative $M_6ZX_{12}L_6$ cluster geometry of relevance here has been encountered in a few compounds. As shown at the right in Fig. 2, the metal atoms in this geometry surround the interstitial atom Z to form a trigonal prism instead of an octahedron. Twelve edge-bridging anions X complete the cluster core, with two bridging each of the longer edges of the trigonal prism, and one bridging each of the shorter edges. Here again, a single terminal ligand L extends from

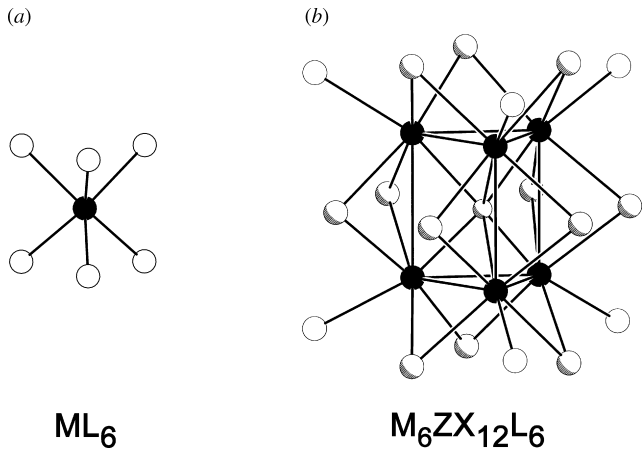

Figure 2. Idealized structures of a trigonal prismatic ML_6 complex (*a*) and a centered edge-bridged trigonal-prismatic $M_6ZX_{12}L_6$ cluster (*b*). Black, small shaded, large shaded, and white spheres represent metal atoms M, interstitial atom Z, inner ligands X, and terminal ligands L, respectively. Each structure conforms to D_{3h} symmetry.

each metal vertex, now resulting in an outer ligand set akin to that of a trigonal prismatic ML_6 complex. Note that the nonmetal atoms of the cluster are arranged in a hexagonal closest packing, whereas those of the centered, edge-bridged octahedral geometry are arranged in a cubic closest packing. Trigonal-prismatic clusters of this type were first observed within the one-dimensional (1D) compounds $A_3Nb_6SBr_{17}$ (A = K, Rb, Cs, Tl) (28, 29). Very recently, they have also been observed in the two-dimensional (2D) solid W_6CCl_{16} and as the molecular species $[W_6CCl_{18}]^{n-}$ ($n = 0$–3) and $[W_6NCl_{18}]^{n-}$ ($n = 1-3$) (30–32). Taking $[W_6CCl_{18}]^{2-}$ as a prototype, it is worth noting that mean $Cl^a\cdots C\cdots Cl^a$ angles of 71.7° and 89.2° deviate somewhat from the analogous S—Mo—S angles of 78.7° and 84.0° in MoS_2 (33, 34). While trigonal-prismatic technetium and rhenium halide clusters are known without interstitial atoms, these have multiple-bond character along three parallel edges, leading to an outer ligand arrangement that is unlike that of any simple metal complex (34).

B. Electronic Structures

The electronic structures for many hexanuclear clusters adopting the basic geometries displayed in Figs. 1 and 2 have been investigated using a variety of computational methods (30, 35–47). We will therefore only briefly summarize the results obtained from DFT calculations performed—by methods described in detail elsewhere (30, 44, 45)—on a few representative examples.

The frontier orbitals calculated for the face-capped octahedral cluster $[Re_6Se_8Cl_6]^{4-}$ consist of a pair of e_g highest occupied molecular orbitals (HOMOs) and an a_{2g} lowest unoccupied molecular orbitals (LUMO), as shown in the middle of Fig. 3. The former are primarily rhenium–rhenium bonding in character, with some rhenium–selenium antibonding contributions, while the latter is almost exclusively rhenium–rhenium antibonding in character. The 10 orbitals (three triply degenerate orbital sets and an a_{1g} orbital) directly lower in energy than the HOMO are principally rhenium–rhenium bonding in character. This result is quite analogous to that obtained previously for the face-capped octahedral Mo_6S_8 units of the Chevrel phases (38). Filling 12 rhenium–rhenium bonding orbitals with 24 electrons gives the equivalent of a single two-center, two-electron bond per Re—Re edge of the Re_6 octahedron; thus, the cluster is electron precise. Consistent with the expectation that all of these bonding orbitals should be filled, the cluster formally contains Re(III), affording a count of $6 \times 4 = 24$ metal-based valence electrons. While the majority of the face-capped octahedral clusters have this preferred electron count of 24, counts as low as 19 and as high as 25 have been established within Nb_6I_{11} and $[Re_4Os_2Se_8(CN)_6]^{3-}$, respectively (20, 45). Since the HOMO for $[Re_6Se_8Cl_6]^{4-}$ is doubly degenerate, one would expect the one-electron oxidized (23-electron) cluster to undergo a first-order Jahn–Teller distortion. Indeed, careful examination of

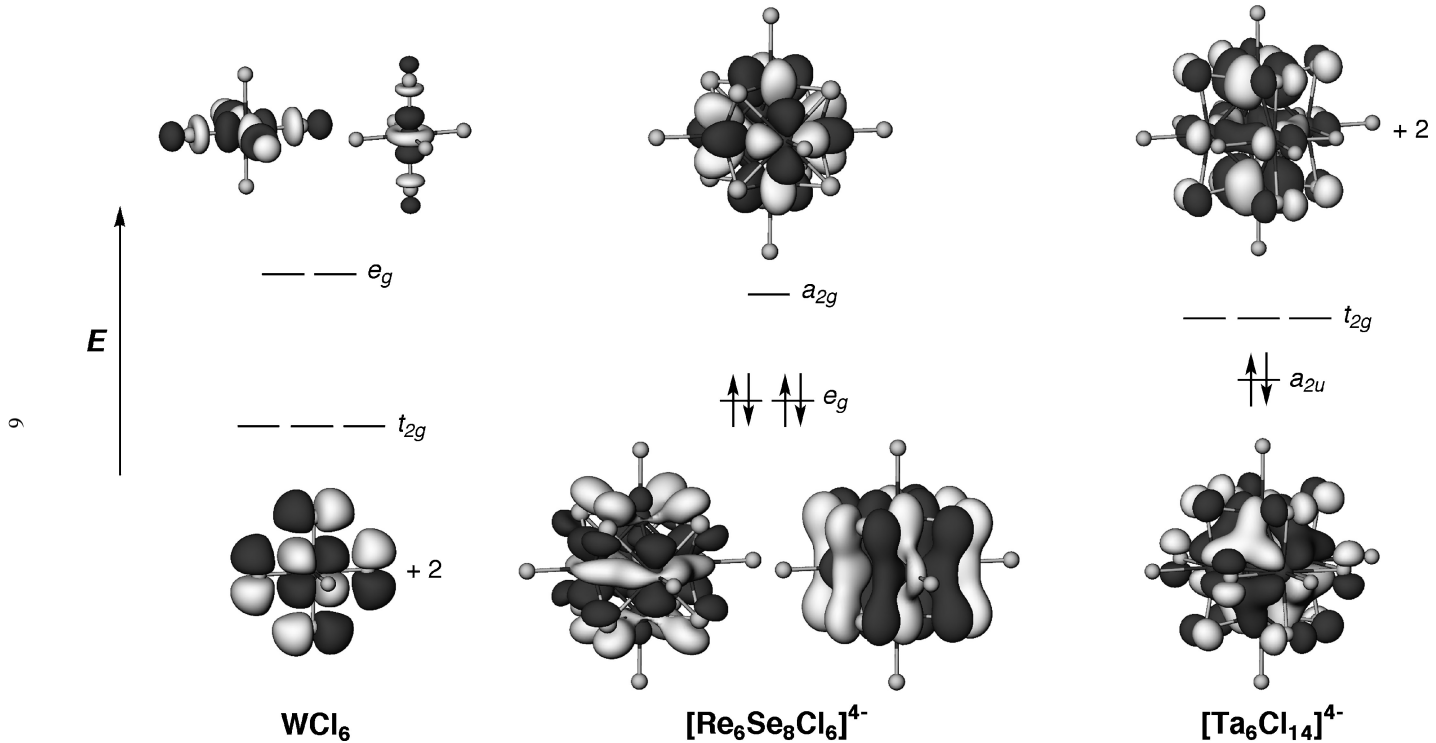

Figure 3. Frontier orbitals for WCl_6, $[Re_6Se_8Cl_6]^{4-}$, and $[Ta_6Cl_{14}]^{4-}$, representing the octahedral ML_6, face-capped octahedral $M_6X_8L_6$, and edge-bridged octahedral $M_6X_{12}L_6$ structure types, respectively. Filling through the e_g orbitals of $[Re_6Se_8Cl_6]^{4-}$ produces a 24-electron cluster, and through the a_{2u} orbital of $[Ta_6Cl_{14}]^{4-}$, a 14-electron cluster.

crystal structures containing $[Re_6X_8(CN)_6]^{3-}$ (X = S, Se) reveals small distortions, consistent with the character of the e_g HOMOs depicted in Fig. 3 (48). Jahn–Teller distortions of similar magnitude have been observed in the 21-electron clusters $[Mo_6X_8(PEt_3)_6]^-$ (X = S, Se) (49), and a considerably more dramatic distortion is apparent in the structure of the trigonal-prismatic clusters $[W_6CCl_{18}]^{3-}$ and $[W_6NCl_{18}]^{3-}$ (30,32). Note that the energy level diagrams for the 24-electron clusters $[M_6X_{14}]^{2-}$ (M = Mo, W; X = Cl, Br, I) differ somewhat from those of the rhenium chalcohalide clusters, exhibiting a t_{2u} HOMO, as was first suggested based on a qualitative analysis of metal orbitals by Gray and co-workers (50).

Edge-bridged octahedral $M_6X_{12}L_6$ clusters are comparatively electron deficient and have fewer electrons involved in metal–metal bonding. The frontier orbitals calculated for $[Ta_6Cl_{18}]^{4-}$ consist of an a_{2u} HOMO and a set of three t_{2g} LUMOs, as shown at the right in Fig. 3. The former is primarily tantalum–tantalum bonding in character, with some tantalum–chlorine antibonding contributions, while the latter exhibit tantalum–chlorine antibonding character and are almost nonbonding for the net tantalum–tantalum interactions. Hyperfine splitting in the electron paramagnetic resonance (EPR) spectrum of the related one-electron oxidized cluster $[Nb_6Cl_{18}]^{3-}$ supports the metal-based nature of the a_{2u} HOMO (51). Below the HOMO lie t_{2g}, t_{1u}, and a_{1g} orbitals that are also principally tantalum–tantalum bonding in character. Thus, the electron filling is in agreement with the count of 16 metal-based valence electrons associated with the six $Ta^{2.33+}$ centers of the cluster. This preference for 16 electrons gives the equivalent of a single three-center, two-electron bond per triangular face of the Ta_6 octahedron. Note, however, that the calculations indicate a large gap between the HOMO and the t_{2g} orbital directly lower in energy, accounting for the stability of oxidized clusters of this type with as few as 14 electrons. Higher electron counts of 17 and 18 have also been established for this geometry in the group 6 clusters $[W_6Cl_{18}]^{1+,0}$ (25, 26, 52).

Incorporation of a central interstitial atom provides a means by which group 4 metals such as zirconium can attain electron counts sufficient to accommodate the edge-bridged octahedral geometry (5, 6, 10). Analysis of the electronic structure of main group element-stabilized clusters indicates mixing of the valence s and p orbitals of the interstitial atom into the metal–metal bonding orbitals of a_{1g} and t_{1u} symmetry. The result is a dramatic stabilization of these framework bonding orbitals that can be construed as donation of the interstitial valence electrons to the electron-deficient metal scaffold. Incorporation of an interstitial transition metal atom has a similar, albeit less dramatic, effect, resulting in a stabilization of the a_{1g} and t_{2g} orbitals with metal–metal bonding character.

For comparison, the frontier orbitals of the single-metal complex WCl_6 are depicted at the left in Fig. 1. Of particular significance is the much

greater contribution of the outer ligands to the composition of these orbitals. Indeed, for the preferred electron counts shown, the frontier orbitals of the octahedral clusters show little or no involvement of the outer chloride ligands. This of course has implications for the ability of their paramagnetic derivatives to participate in magnetic exchange interactions. As discussed below, substitutions at the outer-ligand sites can, however, greatly impact the electronic properties of the clusters.

The electronic structure of the trigonal-prismatic cluster $[Nb_6SBr_{18}]^{4-}$ has also been the subject of a detailed analysis (28). This cluster exhibits only weak niobium–niobium bonding along the longer (3.28 Å) rectangular edges of the Nb_6 trigonal prism, originating in the a_1 HOMO, and somewhat stronger niobium–niobium bonding along its shorter (2.97 Å) edges. Indeed, the two Nb_3 triangular units are held together largely through strong niobium–sulfur interactions, which appear to direct the cluster to the trigonal-prismatic geometry. Interestingly, the first indication of a trigonal-prismatic sulfur-centered unit was observed in the structure of Nb_6I_9S where the sulfur atom resides between nearly eclipsed faces of adjacent Nb_6 octahedra (53).

II. SOLID-STATE SYNTHESIS

The majority of the hexanuclear cluster cores considered here are initially synthesized through high-temperature solid-state routes. To prevent oxide formation, the preparations generally require the use of an evacuated, sealed ampule, the composition of which is dependant on reaction conditions. Procedures requiring temperatures $<500°C$ can employ inexpensive borosilicate reaction vessels, whereas higher temperatures require a more robust material, such as fused silica. In cases where reactions with the glass might occur, tubes made from relatively inert metals, most often niobium or tantalum, are utilized (54). An argon plasma arc welder is usually employed in sealing ampules made from these highly refractory metals. The cluster-forming reactions typically involve the reduction of a transition metal-chalcogenide or -halide featuring the metal in a high oxidation state. A variety of reducing agents have been successfully employed, including the metal–halides and –chalcogenides in lower oxidation states and various highly reducing metals in their elemental states. The most commonly utilized reducing agent, however, is the elemental transition metal itself, in which case there are no redox byproducts that need to be separated from the product mixture. Most solid-state preparations of cluster-containing solids are carried out for several days at temperatures in excess of 700°C.

Cluster formation under such conditions is still poorly understood. Thus far, perhaps the most complete glimpse of a cluster nucleation process was granted in the investigation of a lower temperature route to tungsten iodide clusters (55).

Owing to the inertness of tungsten metal even at high temperatures, $W(CO)_6$ was studied as an alternative source of tungsten atoms. Its reaction with I_2 at 140°C was found to liberate CO gas to give an amorphous black tungsten iodide phase. By further heating this first-formed product to higher and higher temperatures, a series of clusters with increasing nuclearities was established. The results suggest that, at least under these conditions, the pathway to the face-capped octahedral cluster is $[W_3I_9]^{1-} \rightarrow [W_4I_{11}]^{1-} \rightarrow [W_5I_{13}]^{1-} \rightarrow [W_6I_{14}]^{2-}$.

The cluster-containing solids produced under more standard high-temperature conditions tend to feature the clusters locked within an extended network (see Table I). For example, Mo_6Cl_{12} exhibits a 2D structure, in which each face-capped octahedral $[Mo_6Cl_8]^{4+}$ cluster core has two trans terminal chloride ligands (Cl^a), while the other four outer chloride ligands form bridges to a neighboring cluster core ($Cl^{a\text{-}a}$) (see Fig. 4). Only van der Waals interactions occur between the ensuing chloride-bridged sheets, such that bringing the clusters into solution would require a reagent capable of cleaving, on average, two Mo—Cl bonds per cluster. In many instances, the connections between cluster cores are even tighter, which is the case for $Re_6Se_8Cl_2$. This compound has a 2D structure similar to that of Mo_6Cl_{12}, but with rhombic Re_2Se_2 interactions directly linking the face-capped

TABLE I
Parent Solids Formed by High-Temperature Solid-State Routes

Compound	e^- Count	Connectivity (33)	Dimensionality	References
Zr_6HCl_{12}	13	$[Zr_6H\mathrm{Cl}^i_6\mathrm{Cl}^{i-a}_{6/2}]\mathrm{Cl}^{a-i}_{6/2}$	3D	56
Zr_6BeCl_{12}	14	$[Zr_6Be\mathrm{Cl}^i_6\mathrm{Cl}^{i-a}_{6/2}]\mathrm{Cl}^{a-i}_{6/2}$	3D	57
Zr_6BX_{12} (X = Br, I)	15	$[Zr_6B\mathrm{X}^i_6\mathrm{X}^{i-a}_{6/2}]\mathrm{X}^{a-i}_{6/2}$	3D	58
Zr_6CI_{12}	16	$[Zr_6C\mathrm{I}^i_6\mathrm{I}^{i-a}_{6/2}]\mathrm{I}^{a-i}_{6/2}$	3D	59
Zr_6MnI_{12}	19	$[Zr_6Mn\mathrm{I}^i_6\mathrm{I}^{i-a}_{6/2}]\mathrm{I}^{a-i}_{6/2}$	3D	60
Nb_6F_{15}	15	$[Nb_6\mathrm{F}^i_{12}]\mathrm{F}^{a-a}_{6/2}$	3D	61
Nb_6Cl_{14}	16	$[Nb_6\mathrm{Cl}^i_{10}\mathrm{Cl}^{i-a}_{2/2}]\mathrm{Cl}^{a-i}_{2/2}\mathrm{Cl}^{a-a}_{4/2}$	3D	62
Nb_6I_{11}	19	$[Nb_6\mathrm{I}^i_8]\mathrm{I}^{a-a}_{6/2}$	3D	20
Nb_6HI_{11}	20	$[Nb_6H\mathrm{I}^i_8]\mathrm{I}^{a-a}_{6/2}$	3D	20, 21
Ta_6X_{15} (X = Cl, Br)	15	$[Ta_6\mathrm{Cl}^i_{12}]\mathrm{Cl}^{a-a}_{6/2}$	3D	63
Ta_6I_{14}	16	$[Ta_6\mathrm{I}^i_{10}\mathrm{I}^{i-a}_{2/2}]\mathrm{I}^{a-i}_{2/2}\mathrm{I}^{a-a}_{4/2}$	3D	64
$A_xMo_6X_8$ (X = S, Se)	20–24	$[Mo_6\mathrm{Q}^i_2\mathrm{Q}^{i-a}_{6/2}]\mathrm{Q}^{a-i}_{6/2}$	3D	16–19
Mo_6X_{12} (X = Cl, Br, I)	24	$[Mo_6\mathrm{X}^i_8]\mathrm{X}^a_4\mathrm{X}^{a-a}_{4/2}$	2D	65
W_6X_{12} (X = Cl, Br, I)	24	$[W_6\mathrm{X}^i_8]\mathrm{X}^a_4\mathrm{X}^{a-a}_{4/2}$	2D	65
W_6Cl_{18}	18	$[W_6\mathrm{Cl}^i_{12}]\mathrm{Cl}^a_6$	0D	25
W_6CCl_{16}	24	$[W_6C\mathrm{Cl}^i_{12}]\mathrm{Cl}^a_2\mathrm{Cl}^{a-a}_{4/2}$	2D	31
W_6CCl_{18}	22	$[W_6C\mathrm{Cl}^i_{12}]\mathrm{Cl}^a_6$	0D	31
$Re_6S_8X_2$ (X = Cl, Br)	24	$[Re_6\mathrm{S}^i_4\mathrm{S}^{i-a}_{2/2}]\mathrm{X}^a_{4/2}\mathrm{S}^{a-i}_{2/2}$	3D	66, 67
$Re_6Se_8Cl_2$	24	$[Re_6\mathrm{Se}^i_4\mathrm{Se}^{i-a}_{4/4}]\mathrm{Cl}^a_2\mathrm{Se}^{a-i}_{4/2}$	2D	68–72
$Re_6Se_8Br_2$	24	$[Re_6\mathrm{Se}^i_4\mathrm{Se}^{i-a}_{2/2}]\mathrm{Br}^a_{4/2}\mathrm{Se}^{a-i}_{2/2}$	3D	73

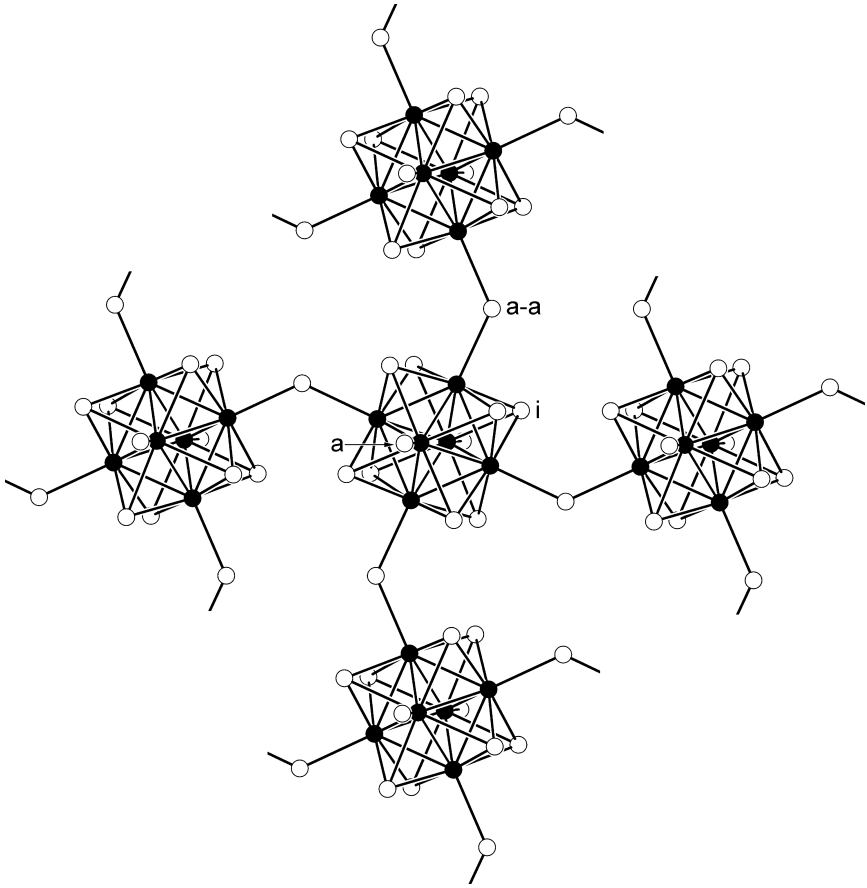

Figure 4. A portion of the structure of Mo_6Cl_{12}, featuring face-capped octahedral cluster cores linked in 2D through bridging outer chloride ligands (65). Black and white spheres represent Mo and Cl atoms, respectively. This structure type is shared by Mo_6X_{12} (X = Br, I) and Mo_6Cl_{12} (X = Cl, Br, I).

octahedral cluster cores (as shown at the top of Fig. 5). Here, an inner ligand from a neighboring core also serves as an outer ligand, and liberating the clusters into solution would require cleaving, on average, four Re—Se bonds per cluster. In addition, little space is available for the approach of a bridge-displacing ligand. Accordingly, solution-based reagents are generally not effective in solubilizing such tightly connected frameworks. Instead, one may turn to solid-state approaches, such as that encompassed by dimensional reduction.

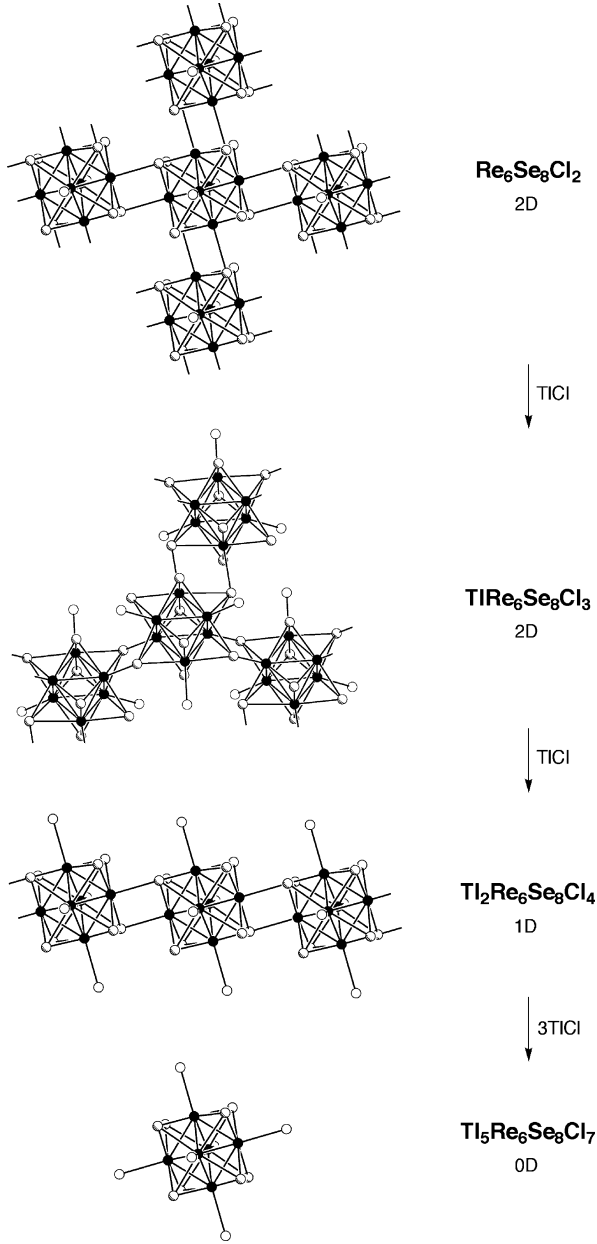

Figure 5. Dimensional reduction of $Re_6Se_8Cl_2$ via incorporation of TlCl. Black, shaded, and white spheres represent Re, Se, and Cl atoms, respectively. Each added equivalent of TlCl supplies another terminal chlorine ligand, reducing connectivity.

A. Dimensional Reduction

1. Standard Salt Incorporation

Dimensional reduction has been set forth as a general method for dismantling noncluster metal–halide and –chalcogenide frameworks in a controlled, predictive manner (74). In such a reaction, a binary parent compound ML_l is heated with n equivalents of a dimensional reduction agent A_aL, where A is significantly more electropositive than M.

$$ML_l + nA_aL \rightarrow A_{na}ML_{l+n} \quad (1)$$

The additional anions X are thereby incorporated into the covalent M—X framework, while the cations A, having weaker ionic interactions with the anions, are treated as residing outside the framework. The resultant child compound $A_{na}ML_{l+n}$ has more anions per metal center, reducing the need for M—L—M bridging interactions. With fewer such bridges, its framework assumes a less tightly connected structure, often one that represents a lower dimensional fragment of the original parent framework. Ultimately, with the introduction of sufficient A_aL, all bridges are terminated to produce a simple molecular salt. Thus, for example, reaction of the three-dimensional (3D) compound VF_3 with 3 equiv of LiF at 700°C affords Li_3VF_6, featuring octahedral the octahedral complex $[VF_6]^{3-}$ (75).

Dimensional reduction can be applied similarly in breaking up many of the hexanuclear cluster-containing solids listed in Table I. Here, in place of single metal centers, it is the cluster cores that retain their structure and redox state through the course of the reaction:

$$M_6X_xL_l + nA_aL \rightarrow A_{na}M_6X_xL_{l+n} \quad (2)$$

As before, the more A_aL incorporated into the structure, the less connected the ensuing framework will be. The results are exemplified in Fig. 5 with a sequence of child compounds derived from $Re_6Se_8Cl_2$ (76). A high-temperature reaction incorporating a single equivalent of TlCl affords $TlRe_6Se_8Cl_3$, in which each cluster has one additional terminal chloride ligand. Note that, while the overall dimensionality of the framework remains at two, the average number of Re—Se bonds that must be cleaved to release the clusters into solution has been reduced from four per cluster to three per cluster. Addition of one further equivalent of TlCl gives the 1D compound $Tl_2Re_6Se_8Cl_4$, featuring four terminal chloride ligands per cluster. Finally, incorporation of five total equivalents of TlCl produces the molecular salt $Tl_5Re_6Se_8Cl_7$ ($= Tl_4Re_6Se_8Cl_6 \cdot TlCl$), in which every cluster has a full compliment of six terminal chloride ligands. Note that, in all of

these phases, the $[Re_6Se_8]^{2+}$ cluster cores maintain both their face-capped octahedral geometry and their preferred count of 24 metal-based valence electrons. Further note that, since these are thermodynamically stable products, one need not follow the reaction sequence layed out in Figure 5, and can simply target the desired phase directly through a stoichiometric, high-temperature reaction. Related reactions employing cesium halides as dimensional reduction agents have provided water-soluble cesium salts of the clusters $[Re_6X_8L_6]^{4-}$ (X = S, L = Cl, Br, I; X= Se, L = I), opening the way to a remarkably rich solution chemistry (13).

Other examples of compounds related to cluster-containing parent solids through dimensional reduction are enumerated in Table II. In a few instances, child compounds are also listed for a hypothetical, but chemically reasonable parent phase (as designated by quotation marks around the chemical formula). Note that many of the child compounds correspond to molecular cluster salts, which when incorporating exclusively alkali metal cations are generally soluble in highly polar solvents. Indeed, of the 24 distinct cluster cores occurring in the nonmolecular parent phases listed in Table I, 10 have thus far been rendered into a soluble molecular form via dimensional reduction. Of particular interest amongst the remaining 14 cluster cores are $[Zr_6ZI_{12}]$ (Z = C, Mn), $[Nb_6I_8]^{3+}$, and $[Nb_6HI_8]^{3+}$, which do not yet exist in any soluble form (100).

2. *Core Anion Substitution*

Cluster-containing frameworks provide an adjustable parameter not present in simple metal–anion frameworks, since the composition of the cluster core itself can be varied. This enables alteration of the core charge as an alternative means of counterbalancing the charge of the additional terminal ligands. The most straightforward method for effecting such a change is through substitution at one or more of the core anion sites. A frequently occurring example of this involves exchanging a core chalcogenide anion for two halide anions, one filling the vacancy left by the chalcogenide, and one adding to the outer ligand set. Such a substitution results in a lowering of the framework connectedness, without incorporation of a charge balancing cation A.

Beginning again with the 2D parent phase $Re_6Se_8Cl_2$ (see Fig. 5, top), the sequence of child compounds obtained upon substituting two chloride anions for a selenide anion is delineated along the top row of Scheme 1. The first substitution gives $Re_6Se_7Cl_4$, a compound that has been synthesized, but not structurally characterized (101), and is expected to incorporate face-capped octahedral $[Re_6Se_7Cl]^{3+}$ cluster cores. A second substitution yields $Re_6Se_6Cl_6$, a 2D compound adopting the Mo_6Cl_{12} structure (see Fig. 4), with $[Re_6Se_6Cl_2]^{4+}$ cluster cores in place of $[Mo_6Cl_8]^{4+}$ cores (102). A 1D solid, $Re_6Se_5Cl_8$ (102), featuring $[Re_6Se_5Cl_8]^{5+}$ cluster cores surrounded by four terminal chlorides and two

TABLE II
Examples of Compounds Related via Standard Dimensional Reduction

Parent[a]	Child Compound	Dimensionality	References
Zr_6HCl_{12}	$Li_6Zr_6HCl_{18}$	0D	77
Zr_6BeCl_{12}	$K_3Zr_6BeCl_{15}$	3D	78
	$A_4Zr_6BeCl_{16}$ (A = Na, Cs)	2D	57, 79
"Zr_6BeBr_{12}"	KZr_6BeBr_{13}		57
Nb_6Cl_{14}	$A_4Nb_6Cl_{18}$ (A = Li, Na, K, Cs, In, Tl)	0D	80–82
	$Li_2In_2Nb_6Cl_{18}$	0D	83
	$K_2SrNb_6Cl_{18}$	0D	84
	$ARNb_6Cl_{18}$ (A = alkali metal(I), In, Tl, R = rare earth(III), Ti^{III}, V^{III})	0D	85
	$A_2RNb_6Cl_{18}$ (A = alkali metal(I), In, Tl, R = Yb^{II}, V^{II})	0D	86, 87
Nb_6Br_{14}	$ARNb_6Br_{18}$ (A = alkali metal(I), In, Tl, R = rare-earth(III), Ti^{III}, V^{III})	0D	85
	$A_2RNb_6Br_{18}$ (A = alkali metal(I), Tl, R = Eu^{II}, Yb^{II})	0D	88
	$A_4Nb_6Br_{18}$ (A = K, Rb)	0D	89
Ta_6Cl_{14}	$ARTa_6Cl_{18}$ [A = K, Rb, Cs, R = rare earth(III)]	0D	85
Mo_6Cl_{12}	AMo_6Cl_{13} (A = Na, Ag)	1D	90
	AMo_6Cl_{14} (A = Mg, Ca, Sr, Ba, V-Ni, Cd, Sn, Pb, Yb, Eu)	0D	90
	$A_2Mo_6Cl_{14}$ (A = Li, K, Rb, Cs, Cu)	0D	90
Mo_6Br_{12}	$SnMo_6Br_{14}$	0D	91
	$Cu_2Mo_6Br_{14}$	0D	92
Mo_6I_{12}	$Cu_2Mo_6I_{14}$	0D	92
KMo_6Se_8	$K_6Mo_6Se_8(CN)_5$	1D	93
	$K_7Mo_6Se_8(CN)_6$	0D	94
W_6Br_{12}	CdW_6Br_{14}	0D	95
	$Cu_2W_6Br_{14}$	0D	96
"Re_6S_9"	$Li_4Re_6S_{11}$	3D	97
	$A_{10}Re_6S_{14}$ (A = Rb, Cs)	0D	98
$Re_6S_8Cl_2$	$A_2Re_6S_8Cl_4$ (A = Tl, Cs)	1D	76
	$A_5Re_6S_8Cl_7$ (A = Tl, Cs)	0D	76
	$Cs_{2.87}K_{1.13}Re_6S_8Cl_6$	0D	99
$Re_6S_8Br_2$	$Cs_5Re_6S_8Br_7$	0D	13
"$Re_6S_8I_2$"	$Cs_6Re_6S_8I_8$	0D	13
$Re_6Se_8Cl_2$	$TlRe_6Se_8Cl_3$	2D	76
	$Tl_2Re_6Se_8Cl_4$	1D	76
	$Tl_5Re_6Se_8Cl_7$	0D	76
$Re_6Se_8Br_2$	$Cs_2Re_6Se_8Br_4$	1D	13
	$Cs_5Re_6Se_8Br_7$	0D	13
"$Re_6Se_8I_2$"	$CsRe_6Se_8I_3$	2D	13
	$Cs_4Re_6Se_8I_6$	0D	13

[a]Parent compounds listed in quotation marks are not yet known.

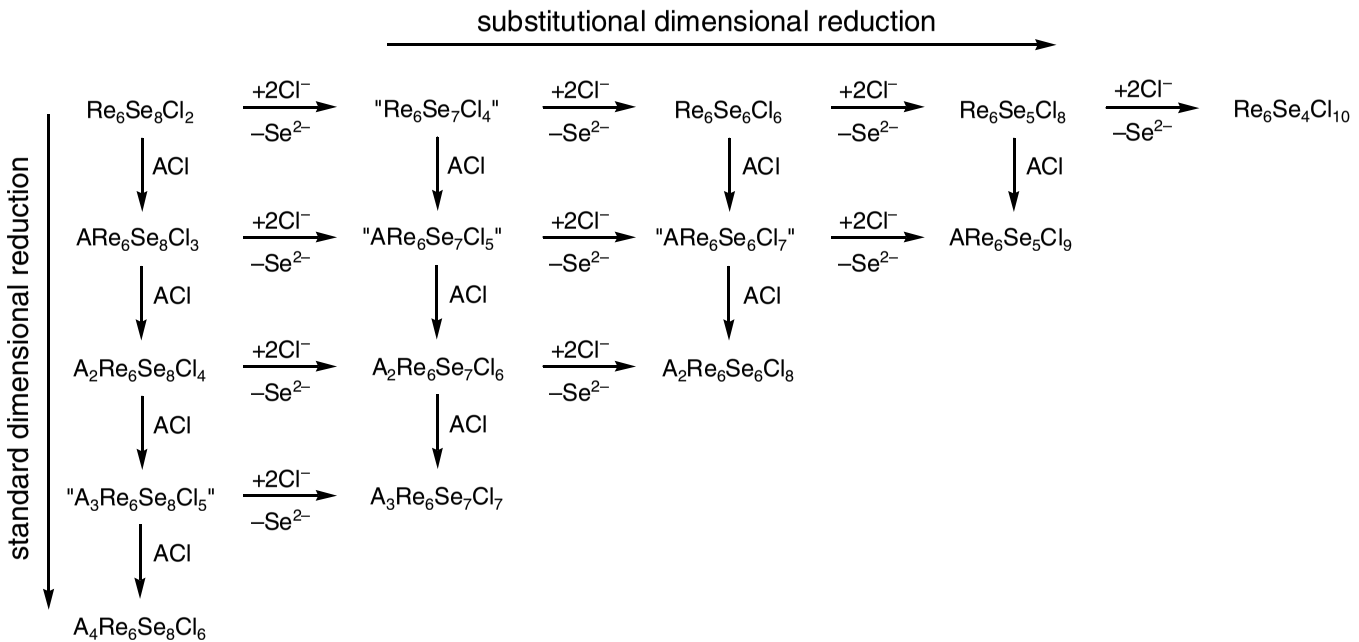

Scheme 1. Examples of compounds not listed in quotation marks have been synthesized and structurally characterized.

bridging chlorides, results from a third such substitution. Finally, four total substitutions yield the neutral molecular compound, $Re_6Se_4Cl_{10}$, wherein every $[Re_6Se_4Cl_4]^{6+}$ core is capped by six terminal chloride ligands (103, 104). Each of the foregoing nonmolecular phases can further be treated as a parent, generating the vertical sequences of (grand)child compounds appearing in Scheme 1 via the standard dimensional reduction described in Section 2.A.1. Note that as one moves down and to the right in Scheme 1, the connectedness of the cluster framework decreases, until molecular phases are achieved along the lower right diagonal.

Specific compounds related through substitutions of this type are listed in Table III. The majority of the examples isolated thus far consist of rhenium

TABLE III
Examples of Dimensional Reduction via Core Anion Substitution

Parent	Child Compounds[a]	Dimension	Grandchild Compounds	Dimensionality	References
Nb_6I_{11}	Nb_6SI_9[b]	1D			53
Nb_6HI_{11}	Nb_6HSI_9[b]	1D			53
Mo_6Br_{12}	$Mo_6S_2Br_8$[b]	1D	$Cs_4Mo_6S_2Br_{12}$	0D	105, 106
	"$Mo_6Se_2Br_8$"[b]		$Cs_4Mo_6Se_2Br_{12}$	0D	106
Mo_6I_{12}	$Mo_6X_2I_8$ (X = S, Se)[b]	1D			105
$Re_6S_8Cl_2$	"$Re_6S_7Cl_4$"		$Cs_3Re_6S_7Cl_7$	0D	107
	"$Re_6S_6Cl_6$"		$ARe_6S_6Cl_8$ (A = Mg, Ca, Zn)	0D	108
	$Re_6S_5Cl_8$	1D	$ARe_6S_5Cl_9$ (A = Rb, Ag)	0D	11
	$Re_6S_4Cl_{10}$	0D			109
$Re_6S_8Br_2$	$Re_6S_7Br_4$	3D	$Rb_3Re_6S_7Br_7$	0D	102, 110
	"$Re_6S_6Br_6$"		$K_2Re_6S_6Br_8$	0D	111
	"$Re_6S_5Br_8$"		$ARe_6S_5Br_9$ (A = K, Ag)	0D	112
	$Re_6S_4Br_{10}$	0D			103, 104
$Re_6Se_8Cl_2$	"$Re_6Se_7Cl_4$"		$ZnRe_6Se_7Cl_6$	1D	11
			$Cs_3Re_6Se_7Cl_7$	0D	113
	$Re_6Se_6Cl_6$	2D	$AgRe_6Se_6Cl_7$	1D	11, 102
			$ARe_6Se_6Cl_8$ (A = Mg, Ca, Cd, Pb)	0D	11, 101, 108
			$Cs_2Re_6Se_6Cl_8$	0D	101
	$Re_6Se_5Cl_8$	1D	$ARe_6Se_5Cl_9$ (A = Li, Na, K, Rb, Cu, Ag)	0D	101–103
	$Re_6Se_4Cl_{10}$	0D			103, 104
$Re_6Se_8Br_2$	$Re_6Se_7Br_4$	3D			102, 114
	$Re_6Se_4Br_{10}$	0D			115

[a]Compounds in quotation marks are not yet known.
[b]This child compound is a product of reverse dimensional reduction, and possesses a framework with an increased connectedness relative to its parent structure.

chalcohalide phases containing face-capped octahedral clusters with 24 metal-based valence electrons. All of the other examples represent what might be thought of as reverse dimensional reduction via core anion substitution. In these cases, a core halide anion is replaced with a chalcogenide anion, decreasing the charge of the cluster core by one and thereby eliminating the need for one of the outer halide ligands. This, of course, produces a child compound with a framework that is actually more tightly connected than that of the parent solid. Standard dimensional reduction can then render the resulting new cluster cores soluble, as in the cases of the molecular salts $Cs_4Mo_6X_2Br_{12}$ (X = S, Se). Interestingly, the substitution of chalcogenide anions into edge-bridged octahedral clusters appears to have been little explored, and could provide a fertile area of research. Indeed, many reduced niobium oxyhalide compounds contain edge-bridged octahedral clusters, and fit with this reverse form of substitutional dimensional reduction. These phases have been reviewed elsewhere (4, 9), but are not further considered here, since no parent solid with discrete $[Nb_6O_{12}]^{n+}$ cluster cores is readily formulated.

In addition to anion substitutions that alter the charge of the cluster core, isoelectronic anion substitutions can be made where the charge remains fixed. Here, one type of chalcogenide is replaced with a different chalcogenide, or one type of halide is replaced with a different halide. Obviously, this will not lead to a change in the connectedness of the framework; however, as discussed below, it could influence the basic properties of the resulting cluster. Such substitutions can be accomplished in the usual high-temperature solid-state reactions, simply by introducing a source of the new anion and adjusting the stoichiometry (116). Examples where soluble products have been particularly well-characterized include the clusters $[Mo_6Cl_{8-n}X_nF_6]^{2-}$ (X = Br, I; $n = 0$–8) and $[Re_6Te_{8-n}Se_n(CN)_6]^{4-}$ ($n = 0$–8) (14, 117, 118).

A core anion substitution will generally break the symmetry of the cluster core, and can significantly effect its electronic properties. Consider, for example, the possible substitutions of anions Y into a face-capped octahedral cluster core of generic composition M_6X_8. Recall that the 8 X atoms form a perfect cube [see Fig. 1(*b*)]. The first substitution will simply result in an M_6X_7Y core, for which the symmetry has been lowered to C_{3v}. A second substitution to give an $M_6X_6Y_2$ core, however, will results in three possible isomers: one with the Y atoms sharing a common cube edge (C_{2v}), one with them situated across a face diagonal of the cube (also C_{2v}), and one in which they are situated across a body diagonal of the cube (D_{3d}). A third substitution generates an $M_6X_5Y_3$ core with three possible isomers (one C_{3v} and two C_s), while a fourth generates an $M_6X_4Y_4$ core with seven possible isomers (one T_s, one D_{2h}, one C_{4v}, one C_{3v}, one C_s, and a pair of C_2 enantiomers). Further substitutions simply repeat the pattern with X and Y interchanged. Schematic depictions of all of these isomers can be found in Ref. 114. Substitutions involving atoms with very different electronegativities will of course influence the basic electronic character of

the cluster, skewing its frontier orbitals and, in most instances, creating a dipole moment. In cases, where the charge of the cluster core changes, significant shifts in redox potentials can also occur, as elaborated below. Within a given mixed-anion core composition, different isomers can further be expected to have somewhat different electronic structures; however, these effects have not been investigated in detail, perhaps owing to the difficulties in separating isomers of the same charge.

3. *Heterometal Substitution*

In a very similar way, dimensional reduction can also be carried out through substitutions at the metal sites of a cluster core. This has only recently been demonstrated with the substitution of osmium for rhenium in phases deriving once again from $Re_6Se_8Cl_2$ (113). Here, the strong preference for a count of 24 metal-based valence electrons per face-capped octahedral cluster core dictates that osmium incorporate in the +4 oxidation state. Consequently, with each metal substitution, the charge of the core increases by one, permitting insertion of an additional outer chloride ligand. The products expected through a succession of such substitutions are delineated along the top row of Scheme 2. Of these possibilities, only $Re_4Os_2Se_8Cl_4$, featuring a more loosely connected 2D framework, has yet been isolated and structurally characterized. A number of soluble molecular salts containing mixed-metal clusters have also been obtained by combining heterometal substitution with the standard form of dimensional reduction, specifically $Cs_3Re_5OsSe_8Cl_6$, $Cs_2Re_4Os_2Se_8Cl_4$, and $K_2[Re_3Os_3Se_8Cl_6][Re_4Os_2Se_7Cl_7]$. Numerous other entries in Scheme 1 have yet to be exemplified, including the neutral molecular species $Re_2Os_4Se_8Cl_6$. Note, however, that the substitutions and accompanying increases in core charge here seem to have an even greater influence on the electronic properties of the cluster, such that electrochemical reductions become more and more accessible. Indeed, members of this cluster family have permitted isolation of the first 25-electron face-capped octahedral clusters: $[Re_5OsSe_8(CN)_6]^{4-}$ and $[Re_4Os_2Se_8(CN)_6]^{3-}$ (45). It could be that the most stable redox state for the tetraosmium core is actually $[Re_2Os_4Se_8]^{5+}$, in which case solid-state reactions would better target $Re_2Os_4Se_8Cl_5$ or $KRe_2Os_4Se_8Cl_6$.

Thus far, dimensional reduction has not been applied in this way to any of the other parent solids listed in Table I. Of particular interest are systems that straddle the divide between the edge-bridged and face-centered octahedral geometries. Will reduced niobium–molybdenum halide mixtures simply disproportionate or will they lead to new mixed-metal clusters? If the latter, then where does the crossover in cluster geometries occur? An important factor in applying dimensional reduction is recognizing the variability in the stable electron counts within a particular cluster system. An extreme case occurs

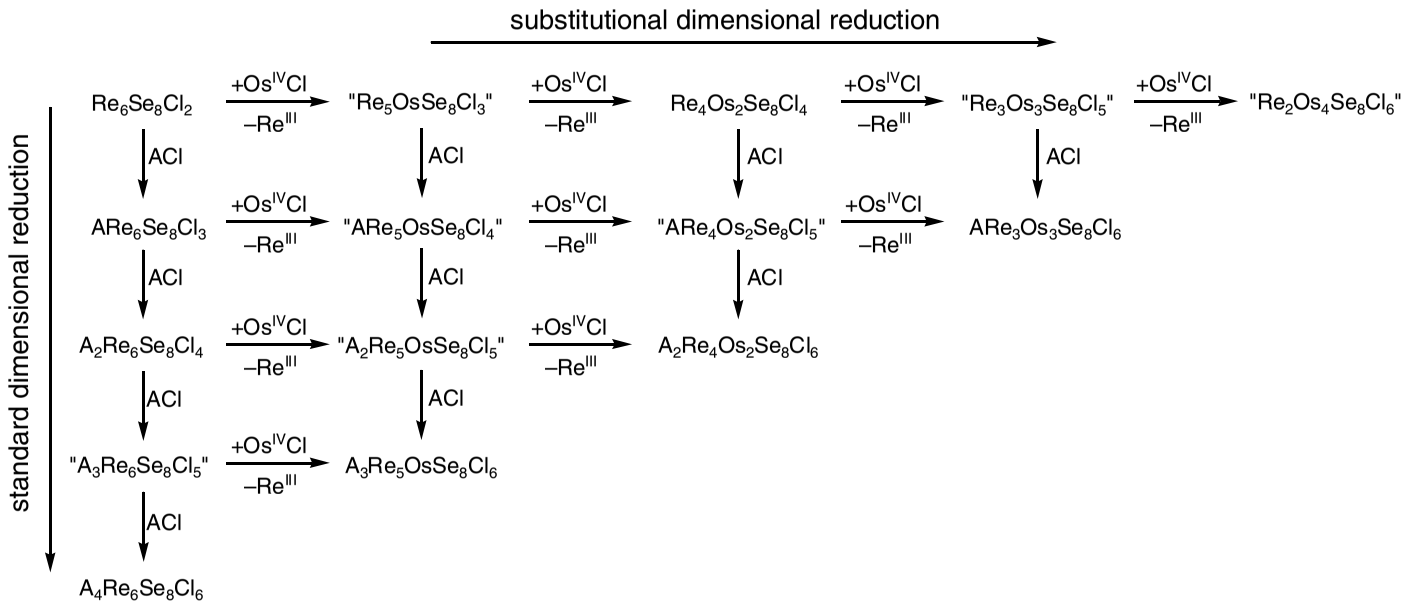

Scheme 2. Examples of compounds not listed in quotation marks have been synthesized and structurally characterized.

with the Chevrel phase parents $A_xMo_6X_8$, for which the number of metal-based valence electrons readily varies between 20 and 24 per cluster. While there are several known mixed-metal Chevrel phase derivatives, specifically the isostructural compounds $Mo_{6-x}M_xX_8$ (M = Re, X = S, Se, Te, $x = 4$; M = Ru, X = Se, Te, $0 \leq x \leq 2$; M = Rh, X = Te, $x = 0.5, 1.33$) (119–123), here the heterometal substitution does not alter the connectivity of the solids, but simply changes the cluster electron count. A similar trend holds for the doubly substituted compounds $Nb_{6-x}Ru_xTe_8$ ($2.50 \leq x \leq 3.17$) (124). In order to effect dimensional reduction in such cases, one likely needs to formulate reactions with cluster electron counts at either of the established limits (here, 20 or 24 electrons).

Very recently, hexanuclear rhenium–molybdenum clusters were obtained by reacting the tetranuclear cluster compound $Re_3MoS_4Te_4$ with KCN at 850°C (125). The resulting crystals of composition $Cs_5Re_{4.5}Mo_{1.5}S_8(CN)_6{\cdot}2H_2O$ are proposed to contain primarily the face-capped octahedral clusters $[Re_5MoS_8(CN)_6]^{5-}$ and $[Re_4Mo_2S_8(CN)_6]^{5-}$, as judged on the basis of crystallographic and energy dispersive spectroscopic analyses. Although the clusters are water soluble, this conclusion has not yet been verified by solution analytical techniques such as nuclear magnetic resonance (NMR) spectroscopy and mass spectrometry. Certainly, this is an interesting and potentially fruitful system for further study.

Isoelectronic heterometal substitutions that do not alter the charge of the cluster core are of course also possible. This will not lead to a change in the connectedness of the framework, but, again, could influence the basic properties of the resulting cluster. Such substitutions can also be accomplished by introducing an appropriate source of the second metal and adjusting the stoichiometry of a high-temperature solid-state preparation. Among the soluble cluster products stemming from reactions of this type, $[Mo_{6-n}W_nCl_8F_6]^{2-}$ ($n = 0 - 6$) and $[Nb_{6-n}Ta_nCl_{12}F_6]^{4-}$ ($n = 1$–5) have been particularly well characterized (126, 127).

Substitution at one or more metal sites will generally break the symmetry of the cluster core, and can greatly influence its electronic properties and reactivity. Consider, for example, the possible substitutions of a metal M′ into an octahedral core of composition M_6X_x ($x = 8, 12$). The first substitution will afford an $M_5M'X_x$ core, for which the symmetry has been lowered to C_{4v}. A second substitution generates an $M_4M'_2X_x$ core with two possible isomers: One in which the M′ atoms are positioned at trans vertices (D_{4h}) and another where they are positioned at cis vertices (C_{2v}). With a third substitution to give an $M_3M'_3X_x$ core, *fac* and *mer* isomers become possible, while further substitutions simply repeat the pattern with M and M' interchanged. Here again, the substitutions can be anticipated to alter the basic electronic properties of the cluster. Moreover, the outer-ligand substitution chemistry could potentially be quite different

for the two metals, as suggested with the isolation of *trans,trans*-$[Re_4Os_2Se_8(PEt_3)_2Cl_4]$ (113). Combining heterometal substitution with core anion substitution of course leads to numerous possible isomers of some complexity; these are enumerated for the face-capped octahedral geometry in reference (113).

4. *Interstitial Substitution*

Parent frameworks featuring hexanuclear clusters stabilized by a central interstitial atom have yet another avenue through which dimensional reduction can be accomplished. In these cases, variation of the interstitial element can be used to manipulate core charge and, in turn, the framework connectedness. The top row of Scheme 3 demonstrates this with application to Zr_6BeCl_{12}, a tightly connected parent phase containing centered, edge-bridged octahedral $[Zr_6BeCl_{12}]^0$ cluster cores with 14 metal-based valence electrons (including two donated by beryllium). Replacing the interstitial beryllium atom with a boron atom yields a $[Zr_6BCl_{12}]^{1+}$ core, enabling incorporation of an outer chloride ligand and loosening the framework. Continuing across the periodic table, substitutions of carbon, nitrogen, and so on, each provide an additional valence electron, increasing by one both the core charge and the number of outer chloride ligands available. For the sake of completeness, this process is continued in Scheme 3 to its resolution, a highly improbable neon-centered molecular cluster. As before, the new phases can themselves serve as parents, and the results of applying the standard form of dimensional reduction are delineated vertically.

Table IV lists specific examples of compounds related through this form of dimensional reduction, By far, the majority of these are zirconium chloride and iodide phases, in which case lower main group and even transition metals have been found to incorporate as interstitial atoms. A few analogues are known with hafnium (135), and very recently it has been shown that nitrogen can be substituted for carbon in tungsten chloride clusters adopting the centered trigonal-prismatic geometry (see Fig. 2) (32). It is hoped that a variability similar to that exposed for the octahedral zirconium clusters will be attainable for such trigonal-prismatic cluster phases.

B. Low-Temperature Routes

Lowering the temperature at which cluster-forming solid-state reactions can be carried out is of some interest, particularly as a means of gaining a measure of kinetic control over the process. Several decades ago, it was discovered that the yields for forming tungsten halide cluster phases could be improved by

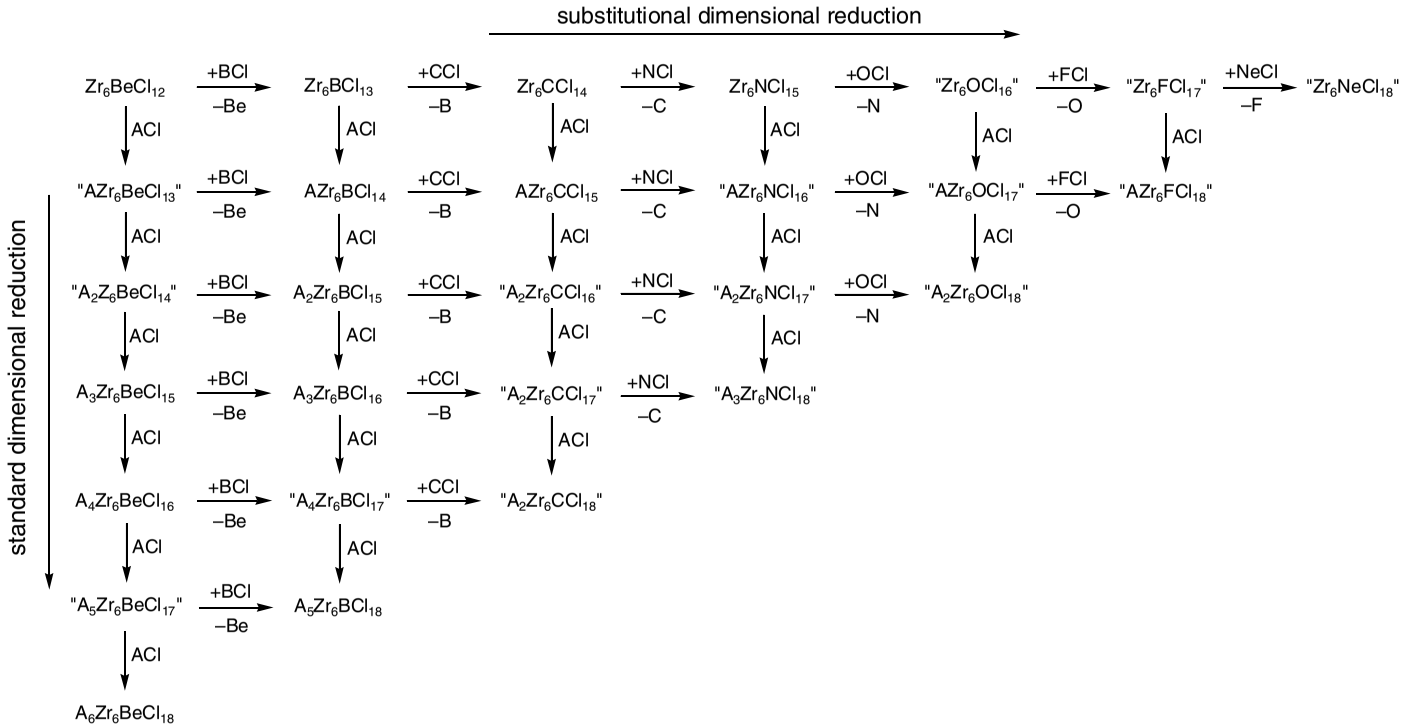

Scheme 3. Examples of compounds not listed in quotation marks have been synthesized and structurally characterized.

TABLE IV
Examples of Dimensional Reduction via Interstitial Substitution

Parent Phase[a]	Child Compound[a]	Dimensionality	Grandchild Compound	Dimensionality	References
Zr_6HCl_{12}	Zr_6BCl_{14}	3D			57
Zr_6BeCl_{12}	Zr_6BCl_{13}	3D	AZr_6BCl_{14} (A = Na, K, Rb, Cs)	3D	57
			$CsKZr_6BCl_{15}$	3D	57
			$A_2Zr_6BCl_{15}$ (A = Na, K)	3D	57
			$Cs_3Zr_6BCl_{16}$	2D	79
			$Ba_2Zr_6BCl_{17}$	1D	128
			$Rb_5Zr_6BCl_{18}$	0D	129
	Zr_6CCl_{14}	3D	AZr_6CCl_{15} (A = K, Rb, Cs)	3D	57, 79
			$Rb_4Zr_6CCl_{18}$	0D	130
	Zr_6NCl_{15}	3D			131
"Zr_6BCl_{12}"	"Zr_6CCl_{13}"		$Cs_3Zr_6CCl_{16}$	2D	79
"Zr_6BeI_{12}"	"Zr_6BI_{13}"		AZr_6BI_{14} (A = K, Cs)	3D	58
	Zr_6CI_{14}	3D			59
Zr_6BI_{12}	"Zr_6CI_{13}"		AZr_6CI_{14} (A = K, Rb, Cs)	3D	59
"Zr_6MgI_{12}"	"Zr_6AlI_{13}"		$Cs_{0.7}Zr_6AlI_{14}$	3D	58
	Zr_6SiI_{14}	3D			132
"Zr_6AlI_{12}"	"Zr_6SiI_{13}"		$Cs_{0.3}Zr_6SiI_{14}$	3D	132
	Zr_6PI_{14}	2D			132
"Zr_6SiI_{12}"	"Zr_6PI_{14}"		$A_xZr_6PI_{14}$ (A = Rb, Cs)	3D	132
"Zr_6CrCl_{12}"	"Zr_6MnCl_{13}"		$CsZr_6MnCl_{14}$	3D	60
			$Li_2Zr_6MnCl_{15}$	3D	133
	"Zr_6FeCl_{14}"		$LiZr_6FeCl_{15}$	3D	133
	Zr_6CoCl_{15}	3D			133
"Zr_6MnCl_{12}"	Zr_6NiCl_{15}	3D			133
"Zr_6CrI_{12}"	"Zr_6MnI_{13}"		$CsZr_6MnI_{14}$	3D	134
	Zr_6FeI_{14}	3D			134
Zr_6MnI_{12}	"Zr_6FeI_{13}"		$CsZr_6FeI_{14}$	3D	134
"Zr_6FeI_{12}"	"Zr_6CoI_{13}"		$Cs_xZr_6CoI_{14}$	3D	134
"Hf_6HCl_{12}"	Hf_6BCl_{14}	3D	$NaHf_6BCl_{15}$		135
"Hf_6BeCl_{12}"	"Hf_6BCl_{13}"		AHf_6BCl_{14} (A = Li, Na, K)		135
	Hf_6CCl_{14}	3D	AHf_6CCl_{15} (A = K, Cs)		135
W_6CCl_{16}	"W_6NCl_{17}"		NaW_6NCl_{18}	0D	32

[a]Compounds in quotation marks are not yet known.

utilizing aluminum metal as a reducing agent in place of tungsten metal (136, 137). Further, these reactions could be carried out at temperatures of just 450°C. More recently, Messerle and co-workers studied the efficacy of a variety of low-melting main group metals in reducing WCl_6, concluding that the best results are obtained with bismuth metal in reactions performed at temperatures as low as 350°C (138). Whether or not these temperatures are truly low enough to permit kinetic control over cluster formation remains to be proven. Regardless, the use of this technique has expanded the library of available W_6 cluster building units considerably.

In one attempt to exercise kinetic control, bismuth metal was used to reduce $WOCl_4$, in the hope that the strong tungsten–oxygen bond might be preserved through the course of the reaction (44). Indeed, work-up of the resulting amorphous black solid enabled isolation of the first hexanuclear tungsten–oxygen–chlorine cluster, $[\alpha\text{-}W_6O_6Cl_{12}]^{2-}$. As depicted on the left in Fig. 6, this species exhibits a structure based upon the edge-bridged octahedral geometry, but with two types of core anions: six chloride anions bridge the edges of two opposing W_3 triangles, while six oxide anions bridge the intervening six edges. The $W—O^i$ bonds are considerably shorter than the $W—Cl^i$ bonds, resulting in a trigonally compressed W_6 octahedron and an overall symmetry of D_{3d}. In analogous reactions performed with excess bismuth, a mixture of products is obtained, including a second D_{3d} isomer, $[\beta\text{-}W_6O_6Cl_{12}]^{2-}$. As shown at the right in Fig. 6, the core chloride and oxide anions are interchanged in this isomer, resulting in a trigonally elongated W_6 octahedron. Separation of the isomers was accomplished by exploiting the differences in the rates of dissolution of the different crystal morphologies associated with the Bu_4N^+ salts of the clusters. Interestingly, both of these structures are consistent with retention of the tungsten–oxygen units of the starting material. Note, however, that some

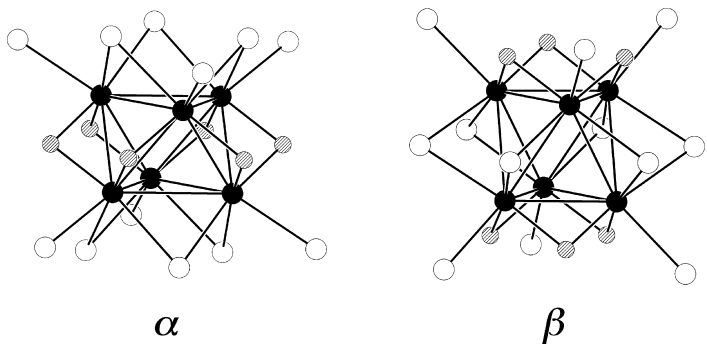

Figure 6. Structures of the two observed isomers of the distorted edge-bridged octahedral cluster $[W_6O_6Cl_{12}]^{2-}$, both with D_{3d} symmetry. Black, hatched, and white spheres represent W, O, and Cl atoms, respectively.

amount of the oxygen-rich cluster $[W_6O_7Cl_{11}]^{3-}$ was also isolated from the products.

Interstitial elements can also be incorporated into clusters through this type of reaction. The concomitant reduction of WCl_6 and CCl_4 with bismuth metal at 400°C generates an amorphous black solid that dissolves in aqueous HCl to liberate $[W_6CCl_{18}]^{2-}$ in 34% yield (30). This carbon-centered cluster adopts the trigonal- prismatic geometry shown in Fig. 2, and has a remarkably rich electrochemistry, with five accessible redox states. Related reactions utilizing NaN_3 in place of CCl_4 afford NaW_6NCl_{18}, a molecular salt containing the analogous nitrogen-centered cluster (32). It is worth noting that the related cluster-containing phases W_6CCl_{16} and W_6CCl_{18} have recently been obtained through standard high-temperature solid-state reactions, albeit in unspecified yield (31).

Although not as problematic as tungsten, reactions using tantalum metal as a reducing agent can also suffer from low yields. While bismuth metal is ineffective at reducing $TaCl_5$, gallium metal is effective, with reactions at 500°C ultimately providing $[Ta_6Cl_{14}]^{2-}$ in high yield (139). Expanding upon this route in ways analogous to those just described for tungsten could provide access to a wide range of new hexanuclear tantalum clusters.

III. SOLUTION METHODS

A. Cluster Excision

For cases where a parent solid is loosely connected, or where dimensional reduction fails to give a molecular salt, solution-based reactions—called excision reactions—can sometimes be used to liberate the clusters into solution (3). In the simplest cases, a polar solvent, such as water, methanol, ethanol, acetonitrile, or dimethylformamide (DMF), is able to disassemble the solid, breaking M—L—M bridges between neighboring clusters to produce a molecular species. Here, a solvent molecule displaces L as a ligand on one of the clusters, yielding M—L + solv—M, such that on average each cluster will have one solvent ligand for every two bridging interactions of this type. As an example, the 2D solid Mo_6Cl_{12} (see Fig. 4) dissolves at least partially upon stirring in a variety of solvents (140–142):

$$Mo_6Cl_{12} + 2\,\text{solv} \rightarrow [Mo_6Cl_{12}(\text{solv})_2] \qquad (\text{solv} = \text{EtOH},\ \text{DMF},\ \text{MeCN},\ \text{etc.}) \tag{3}$$

Excision reactions tend to be low yielding, and can often benefit from the use of Soxhlet extraction techniques. Only a very few excision reactions have beenreported to succeed in dismantling a 3D cluster-containing framework (143–145).

Excision reactions are sometimes accompanied by redox chemistry. For example, dissolution of the 2D solid $Na_4Zr_6BeCl_{16}$ in acetonitrile in the presence of an alkylammonium chloride salt results in simultaneous reduction of the cluster cores (144). Here, the oxidation product remains unidentified, but is presumably the solvent itself. As a means of preventing such redox activity, Hughbanks (6) developed the use of some room temperature molten salts as excision media, specifically with application to centered zirconium–halide cluster phases. A number of these solids have been shown to dissolve in 1-ethyl-2-methylimidazolium chloride–aluminum chloride ionic liquids, providing an efficient route to molecular clusters with a full compliments of terminal chloride ligands. Such molten salts are also well suited for electrochemical studies.

The Chevrel phase Mo_6Se_8 reacts in a KCN melt at 650°C to form both the molecular salt $K_7[Mo_6Se_8(CN)_6]$ (94) and the 1D cyano-bridged compound $K_6[Mo_6Se_8(CN)_5]$ (93, 146). Note that the cluster cores are reduced by one electron in both of these products. The reaction producing a molecular salt has been described as an excision reaction, in which molten KCN acts as the solvent. However, the fact that the latter compound can also be synthesized using a mixture of Mo and $MoSe_2$ in place of Mo_6Se_8, indicates that much more is going on than just the insertion of cyanide ligands between clusters (93). Very likely the cluster units are disintegrating, and, in our view, the reactions are equivalent to a typical solid-state cluster-forming preparation (in which a thermodynamic product is obtained). As such, each of the new compounds can be considered as deriving from a KMo_6Se_8 parent solid via the standard form of dimensional reduction. Indeed, the use of alkali metal cyanide salts as a dimensional reduction agent would seem to offer numerous prospects for forming cyano-bridged cluster frameworks.

B. Solution-Phase Cluster Assembly

Solution-based methods for synthesizing clusters of the type discussed here are of interest as a possible means of exerting kinetic control over product formation. Unfortunately, and perhaps owing to the ease of obtaining the clusters through solid-state reactions, there has been relatively little work in this area. Cotton and co-workers (147, 148) prepared the hydride-stabilized, edge-bridged octahedral cluster $[Zr_6Cl_{18}H_5]^{3-}$ by reduction of $ZrCl_4$ with Bu_3SnH. Initially, this species was thought to be a rare example of a Zr_6 cluster lacking an interstitial atom; however, the presence of five hydride anions was confirmed by time-of-flight neutron diffraction analyses (149). A variation on this self-assembly reaction has further led to isolation of some unique pentanuclear zirconium halide clusters (150). Almost certainly, the development of solution approaches to the synthesis of other hexanuclear clusters would lead to a similar variations in the chemistry.

An elegant approach to producing hexanuclear clusters involves the condensation of two triangular clusters. This was first demonstrated through the reductive dimerization of $[Mo_3S_4Cl_4(PEt_3)_4(MeOH)]$ using magnesium in tetrahydrofuran (THF) to yield the face-capped octahedral cluster $[Mo_6S_8(PEt_3)_6]$ (49, 151). Similarly, $[W_6S_8(PEt_3)_6]$ can be prepared by sequential treatment of $W_3S_7Cl_4$ with PEt_3 and magnesium powder (152). Cross-reactions of this type might, for example, provide a means of synthesizing clusters such as *fac*-$[Mo_3W_3S_8(PEt_3)_6]$ or the C_{3v}-symmetry isomer of $[Mo_6S_4Se_4(PEt_3)_6]$. These intriguing possibilities serve well to illustrate the kind of control feasible with solution assembly reactions.

A recent solution-based cluster-forming reaction reveals something of the limitations for the conditions under which kinetic control can be maintained (153). Reaction of the tetranuclear cluster compound $Re_4Te_4(TeCl_2)_4Cl_8$ with KSeCN and NH_4Cl in acetonitrile superheated to 200°C produces, after 3 days, the face-capped octahedral cluster $[Re_6Se_8(CN)_6]^{4-}$. Here, it is clear from the composition of the rhenium source that this is not simply a condensation reaction, but rather likely involves complete degradation of the original tetrahedral cluster units.

C. Ligand Substitution Reactions

1. Core Anion Exchange

Exchange of core anion ligands via solid-state reactions has already been discussed in the context of substitutional dimensional reduction. Such substitutions can also sometimes be effected in solution; however, given that each anion is bonded to two or three second- or third-row transition metal ions, the activation energy associated with this process is often quite high. Nonetheless, there are several examples of the exchange of core halides for chalcogenides, particularly starting with the 2D solids M_6Cl_{12} (M = Mo, W). Here, dissolution and complete exchange of the core anions is accomplished through reactions with NaSH in the presence of NaBuO and pyridine (py = pyridine, ligand), resulting in formation of the face-capped octahedral clusters $[M_6S_8(py)_6]$ (py = pyridine, ligand) (154). Note that this reaction further involves oxidation of the core from 24 to 20 metal-based valence electrons. Similarly, W_6Cl_{12} reacts with Na_2Se in refluxing pyridine or piperidine to form the analogous clusters $[W_6Se_8L_6]$ (L = py, piperidine) (155, 156). Partial substitution of the inner chloride ligands is also possible, as demonstrated with the near-stoichiometric reactions between Mo_6Cl_{12} and NaSeH to form the 24-electron clusters $[Mo_6SeCl_{13}]^{3-}$ and $[Mo_6Se_2Cl_{12}]^{4-}$ (157, 158).

Preferential substitution of a face-capping chloride ligand over a face-capping chalcogenide ligand can also be accomplished. Reactions between the

mixed-core, face-capped octahedral clusters $[Re_6X_5Cl_9]^{1-}$ (X = S, Se) and silylated $(Me_3Si)_2Y$ reagents produce the clusters $[Re_6X_5YCl_8]^{2-}$ (Y = O, S, Se, Te, NR; R = Me, Bn, $SiMe_3$) (159, 160). Subsequent reaction of $[Re_6X_5(NSiMe_3)Cl_8]^{2-}$ with Bu_4NF affords either the parent imido species $[Re_6X_5(NH)Cl_8]^{2-}$ or, in the presence of MeCl, can form the −NMe or −NBn substituted compounds. Such reactions provide a very interesting means of functionalizing a cluster core, which one can envision as leading to integration of the electronic properties of the cluster with a variety of organic systems.

2. *Terminal Ligand Exchange*

The terminal ligands of a hexanuclear cluster are typically a great deal more labile than its inner-core ligands. There have been numerous studies on substitution reactions involving these ligands, and the results have been reviewed elsewhere in great detail (8). Here, we reemphasize a few of the more generally applicable strategies, and highlight some results that help place cluster cores in the context of expanded analogues of single-metal ions.

Many of the clusters under consideration are first extracted into solution as halide-terminated species of the type $[M_6X_xL_6]^{n-}$ ($x = 8$, 12; L = Cl, Br, I). Such clusters can often be heated in a solvent in the presence of either the acid form or silver(I) salt of a potential anionic ligand, producing the substituted cluster, together with HL or AgL as a stable or even insoluble byproduct. Reactions of this type do not necessarily require that the clusters have a greater affinity for the incoming ligand, and usually an excess of the reactant is sufficient to generate a pure, fully substituted product. Accordingly, this technique provides an effective means of generating cluster complexes with weakly coordinating ligands that are then readily displaced by almost any ligand of choice. Triflate-ligated species in particular are commonly synthesized for this purpose (161–165):

$$[M_6X_xL_6]^{n-} + 6Ag(CF_3SO_3) \rightarrow [M_6X_x(CF_3SO_3)_6]^{n-} + 6AgL \qquad (4)$$

The rate of terminal ligand exchange can vary widely, depending on the nature of the cluster core. As for single metal ions, charge plays a key role, and, with all else being equal, the greater the core charge, the slower the exchange rate can be expected to be. Accordingly, substitution reactions involving the face-capped octahedral core $[W_6S_8]$ are relatively facile, permitting comparison of its binding affinities for a wide range of neutral ligands (166). Using proton nuclear magnetic resonance (^{1}H NMR) spectroscopy, rate constants for self-exchange of the solvent ligand in the clusters $[Re_6Se_8(PEt_3)_5(solv)]^{2+}$ [solv = MeCN, DMSO] at 318 K were determined to be $k = 1.9 \times 10^{-6}$ s^{-1} and 1.6×10^{-6} s^{-1}, respectively (167). These numbers reveal the $[Re_6Se_8]^{2+}$ cluster core to be inert,

with ligand exchange rates comparable to those of a Cr^{3+} or Ru^{3+} ion. Additionally, the activation parameters established in this investigation indicate that the substitutions proceed through a dissociative mechanism with a high-energy barrier. Studies of the kinetics of the exchange of terminal chloride for bromide ligands using ^{36}Cl-labeled $[Mo_6Cl_{14}]^{2-}$ in water revealed that the reaction rate is first order in cluster and independent of the concentration of free chloride ion (168). This suggests a two-step mechanism for the exchange, in which the rate-determining step is an initial substitution of water for the terminal chloride ligands. As one might expect, the rate of the corresponding substitution in $[W_6Cl_{14}]^{2-}$ is significantly slower (169). Further experiments directly comparing outer-ligand exchange rates for a broader spectrum of the available hexanuclear clusters would certainly be of value.

The inertness of the $[Re_6X_8]^{2+}$ (X = S, Se) cores facilitates synthesis of site-differentiated clusters. For these clusters, terminal iodide ligands are more labile than bromide and chloride ligands, which, in turn, are much more labile than triethylphosphine ligands. Starting from $[Re_6S_8Br_6]^{4-}$ or $[Re_6Se_8I_6]^{4-}$, reactions with PEt_3 in hot DMF for varying durations produce members of the cluster families $[Re_6S_8(PEt_3)_nBr_{6-n}]^{(4-n)-}$ and $[Re_6Se_8(PEt_3)_nI_{6-n}]^{(4-n)-}$ (170, 171). A mixture of several species is typically obtained; however, the differences in charge and dipole moment, permit their separation via column chromatography. The isomers obtained for each composition are directly analogous to those enumerated above for octahedral $M_6M'_{6-n}$ clusters. Site-differentiated clusters of this type are expected to be of use as building units in the directed assembly of bridged multiclusters and low-dimensional solids; indeed, as discussed below, some such constructs have already been synthesized (170–178). Notably, *cis*- and *trans*-$[Re_6Se_8(PEt_3)_4I_2]$ and $[Re_6Se_8(PEt_3)_5I]^+$ have all been shown to react with AgCN in solution to replace iodide with cyanide selectively and in good yield (167).

Another means of differentiating the reactivity of terminal ligand sites is through the use of chelating ligands. Recently, the first example of this was reported, with reactions between $[Re_6Se_8I_6]^{3-}$ and $Ph_2PCH_2CH_2CH_2CH_2CH_2CH_2PPh_2$ (dpph) to form the chelate cluster complexes $[Re_6Se_8(dpph)_nI_{6-2n}]^{(4-2n)-}$ ($n = 1$–3) (179). The long backbone of the diphosphine ligand is of course necessary for extension along an edge of the Re_6 octahedron. Note that for clusters with the edge-bridged octahedral geometry, an even longer backbone may be required, owing to both the longer M—M distance and the core anion protruding from each edge (see Fig. 1). Such chelators might be of particular utility in differentiating sites on clusters that rapidly exchange their outer ligands.

In cases where substitutions are extremely slow, high-temperature solid-state reactions can sometimes provide a convenient and efficient means of exchanging outer cluster ligands. Melts of ionic compounds with an anionic component that

can serve as a suitable terminal ligand have been used extensively for this purpose. An illustrative example is the reaction between $Cs_5Re_6S_8Br_7$ or $Cs_4Re_6Se_8I_6$ and an excess of NaCN at 635°C to form the cyano-terminated cluster phases $NaCs_3Re_6X_8(CN)_6$ (X = S, Se) (180). Under similar conditions, the mixed-metal cluster compounds $Cs_3Re_5OsSe_8Cl_6$ and $Cs_2Re_4Os_2Se_8Cl_6$ tend toward disproportionation, forming the related Re_6 clusters and unidentified osmium-containing products. Alkali metal salts of the weakly coordinating anions nitrate and triflate melt at considerably lower temperatures than the corresponding cyanide salts, and can provide an effective solvent for lower temperature exchange reactions. Accordingly, $[Re_5OsSe_8Cl_6]^{3-}$ and $[Re_4Os_2Se_8Cl_6]^{2-}$ react with NaCN in a melt of $NaNO_3$ or KCF_3SO_3 at 320°C to afford the corresponding cyano-substituted species $[Re_5OsSe_8(CN)_6]^{3-}$ and $[Re_4Os_2Se_8(CN)_6]^{2-}$ (45). Relatedly, a KSCN melt at 200°C was recently used to prepare the thiocyanate terminated clusters $[Re_6X_8(NCS)_6]^{4-}$ (X = S, Se) (181).

IV. ELECTRONIC PROPERTIES

A. Electrochemistry

As a result of the close energy spacing and delocalized nature of their frontier orbitals (see Fig. 3), hexanuclear clusters frequently exhibit several chemically accessible redox states. Of the clusters considered here, the most extensive redox series has been observed in cyclic voltammetry experiments performed on solutions of $(Bu_4N)_2[W_6CCl_{18}]$ in DMF (30). Four reversible redox couples are apparent within a 2.4-V window, indicating the accessibility of five redox states of the trigonal-prismatic cluster: $[W_6CCl_{18}]^{(0-4)-}$. Of these, four have been isolated and structurally characterized, and the fifth, $[W_6CCl_{18}]^{4-}$, should be readily generated using a reductant such as sodium metal. Typically, edge-bridged octahedral clusters of zirconium, niobium, or tantalum have three or four accessible redox states (182–186). The clusters $[Mo_6X_8(PEt_3)_6]$ (X = S, Se) also exhibit a rich electrochemistry, with three one-electron transformations accessing sates with 19–22 metal-based valence electrons (49). In contrast, halide-terminated clusters bearing the face-capped octahedral cores $[M_6X_8]^{4+}$ (M = Mo, W; X = Cl, Br, I) and $[Re_6X_8]^{2+}$ (X = S, Se) generally exhibit only one accessible redox change, corresponding to an oxidation to give a 23-electron cluster (187–190).

The most straightforward means of shifting the electrochemistry of a cluster is through substitution of its terminal ligands. For example, exchanging the π-donating chloride ligands of $[Re_6Se_8Cl_6]^{4-}$ (188) for weakly π-accepting cyanide ligands to form $[Re_6Se_8(CN)_6]^{4-}$, results in a shift of the potential for the one-electron oxidation in acetonitrile by +0.51 V (190). This shift is of

course consistent with the core electron density delocalizing to some extent onto the outer ligands. At +0.85 V, the shift is even larger for $[Re_6Se_8(PEt_3)_6]^{2+}$, presumably owing in part to the change in overall charge of the cluster. The changes are also pronounced with even partial substitution of neutral nitrogen-donor ligands such as pyridine for the chloride ligands. Thus, the one-electron oxidation potential in acetonitrile is shifted +0.42 V for $[Re_6S_8Cl_4(py)_2]^{2-}$ and +0.62 V for *mer*-$[Re_6S_8Cl_3(py)_3]^{-}$ versus that of $[Re_6S_8Cl_6]^{4-}$ (191). Here again, the shifts may be related to the changes in the charge of the clusters, as much as to the electronic nature of the ligand.

A core anion substitution can also significantly impact the redox properties of a cluster. For example, the one-electron oxidation of $[Mo_6SeCl_{13}]^{3-}$ in dichloromethane occurs at a potential that is shifted by −0.80 V relative to the analogous oxidation for $[Mo_6Cl_{14}]^{2-}$, making the 23-electron state much easier to access in the former species (192). With one further substitution, oxidation of $[Mo_6Se_2Cl_{12}]^{4-}$ is even more facile, occurring at a potential that is shifted by an additional −0.82 V. Very likely, these shifts are largely a result of the reduction in core charge associated with each successive substitution. Note that the potential quoted for $[Mo_6Se_2Cl_{12}]^{4-}$ is actually an average of the values for two geometrical isomers of the cluster, which differ themselves by 0.07 V (158). An even larger difference is observed for the redox couples of the two mixed-core isomers $[\alpha\text{-}W_6O_6Cl_{12}]^{2-}$ and $[\beta\text{-}W_6O_6Cl_{12}]^{2-}$, with the structures depicted in Figure 6 (44). In acetonitrile solution, each isomer exhibits two reversible one-electron reductions, but these occur at potentials that are 0.15 and 0.08 V more positive for the α isomer than for the β isomer.

Substitutions at the metal sites that alter the core charge can similarly effect cluster redox potentials. For example, the one-electron oxidation of $[Re_5OsSe_8Cl_6]^{3-}$ in acetonitrile occurs at a potential that is 0.74 V more positive than the analogous oxidation for $[Re_6Se_8Cl_6]^{4-}$, while that of $[Re_4Os_2Se_8Cl_6]^{2-}$ is shifted outside the solvent window (113). Here again, the trend is consistent with the increase in core charge making the oxidation more and more difficult. As this occurs, any possible reductions should also become more accessible. Such behavior is indeed observed for the analogous cyano-terminated clusters $[Re_5OsSe_8(CN)_6]^{3-}$ and $[Re_4Os_2Se_8(CN)_6]^{2-}$, which in acetonitrile solution exhibit reversible one-electron reduction waves (45). In the latter case, the potentials for the cis and trans isomers differ significantly, occurring at +1.08 V and +0.81 V, respectively, relative to the $[Re_5OsSe_8(CN)_6]^{3-/4-}$ couple. The diosmium clusters also each exhibit a second one-electron reduction couple, with a comparable difference between the potentials for the two isomers (193). The accessibility of these reductions has enabled isolation and characterization of the first face-capped octahedral clusters with 25 metal-based valence electrons: $[Re_5OsSe_8(CN)_6]^{4-}$ and $[Re_4Os_2Se_8(CN)_6]^{3-}$. For the di- and triosmium clusters, 26-electron species should also be readily attainable.

B. Paramagnetism

The accessible redox chemistry of the clusters in many cases permits isolation of paramagnetic species. Noting the electron configurations presented in Figure 3 for stable diamagnetic clusters, one-electron redox processes can generally be expected to lead to ground states of $S = \frac{1}{2}$. In these cases, the spin will generally be delocalized over the cluster core, with little extension onto the outer ligands. The g values associated with these states can vary considerably from 2. For example, frozen-solution EPR measurements indicate $g = 2.51$ for the 23-electron cluster $[Re_6Se_8I_6]^{3-}$ (172), while $g = 1.46$ for the 25-electron cluster $[Re_5OsSe_8(CN)_6]^{4-}$ (45). Interestingly, the g values for the cis and trans isomers of the related 25-electron cluster $[Re_4Os_2Se_8(CN)_6]^{3-}$ differ considerably, arising at 1.74 and 1.09, respectively. Here, DFT calculations indicate some extension of the spin onto the terminal cyanide ligands, and, indeed, as discussed below, the clusters can participate in weak magnetic exchange interactions (45). Similar capabilities can be anticipated for certain paramagnetic clusters with the edge-bridged octahedral geometry; however, this has not yet been demonstrated. While, on the basis of their electronic structures (194), 12-electron clusters such as $[Zr_6BeCl_{18}]^{4-}$ can be expected to exhibit an $S = 1$ ground state, to our knowledge this has never been proven experimentally.

C. Photochemistry

Luminescence was first discovered in a hexanuclear cluster >20 years ago. The investigation showed the face-capped octahedral cluster $[Mo_6Cl_{14}]^{2-}$ to exhibit one of the longest luminescence lifetimes of any transition metal complex (195). A later study of the related clusters $[M_6X_8L_6]^{2-}$ (M = Mo, W; X, L = Cl, Br, I) revealed each to be luminescent, with a triplet excited state that is quenched by oxygen (15, 196, 197). More detailed studies involving the photosensitized oxidation of 1-methylcyclohexene and 1,2-dimethylcyclohexene verified that the quenching mechanism is an energy-transfer process producing singlet oxygen. As such, the utility of $[Mo_6Cl_{14}]^{2-}$ as an oxygen sensor has been demonstrated by implanting the clusters in fiber optic cables (198).

As suggested by DFT calculations (33, 34) and experimentally verified (189, 199, 200), face-capped octahedral $[Re_6X_8]^{2+}$ (X = S, Se) cluster cores are also luminescent with a variety of terminal ligands. Indeed, a great many examples of these clusters have now been examined, and the results reveal a strong dependence of the luminescence characteristics upon the nature of the outer ligands. Cores terminated by neutral nitrogen- and oxygen-donor ligands have both the longest emission lifetimes and the highest quantum yields, with $[Re_6Se_8(dmso)_6]^{2+}$ exhibiting $\phi_{em} = 24\%$ and $\tau_0 = 22\ \mu s$ (199). Note that, to

our knowledge, all the studies thus far of the photophysical properties of clusters have involved face-capped octahedral cores with homogeneous sets of metal atoms and core anions. Certainly, extension of this work to other cluster types is of interest, and has the potential for extending our understanding of the effects of core structure on luminescence.

V. CLUSTERS AS BUILDING UNITS

As noted previously, the clusters considered here can be viewed as expanded variants of either an octahedral or a trigonal-prismatic transition metal complex (see Figs. 1 and 2). Accordingly, with development of their outer-ligand coordination chemistry to include bridge-forming ligands, they can be utilized equivalently in the solution-based assembly of coordination solids and supramolecular constructs (201, 202). Most importantly, the preceding synthetic methods for manipulating the cluster composition can then be brought to bear in adjusting the properties of the ensuing materials.

A. Extended Solid Frameworks

Owing to their larger size, coordination solids incorporating cluster cores in place of individual metal centers can be expected to have an expanded framework structure. This is of particular interest for 3D solids, wherein the expansion could produce a highly porous framework with host–guest properties similar to those of zeolites.

One of the oldest known coordination solids is Prussian blue, $Fe_4[Fe(CN)_6]_3 \cdot 14H_2O$, a compound exhibiting the cubic 3D structure based upon the unit cell displayed at the left in Fig. 7 (203). The insoluble form of this brilliantly colored pigment is readily prepared by adding ferric ions to an aqueous solution containing the octahedral complex $[Fe(CN)_6]^{4-}$. In a direct parallel, ferric ions react with the face-capped octahedral cluster $[Re_6Se_8(CN)_6]^{4-}$ in aqueous solution to afford a cluster-containing Prussian blue analogue (204):

$$4[Fe(H_2O)_6]^{3+} + 3[Re_6Se_8(CN)_6]^{4-} \rightarrow Fe_4[Re_6Se_8(CN)_6]_3 \cdot 36H_2O \qquad (5)$$

The resulting structure is shown in Figure 7(b), and indeed consists of a direct expansion of Prussian blue, with $[Re_6Se_8]^{2+}$ cluster cores substituted onto all of the Fe^{2+} ion sites. Analogous to the situation in Prussian blue, one out of every four $[Re_6Se_8(CN)_6]^{4-}$ units is missing from the framework, creating large water-filled cavities best envisioned by excising the central cluster from the unit cell. Notably, the volume of the framework cavities and the size of the pore openings have both increased significantly relative to Prussian blue. A range of such

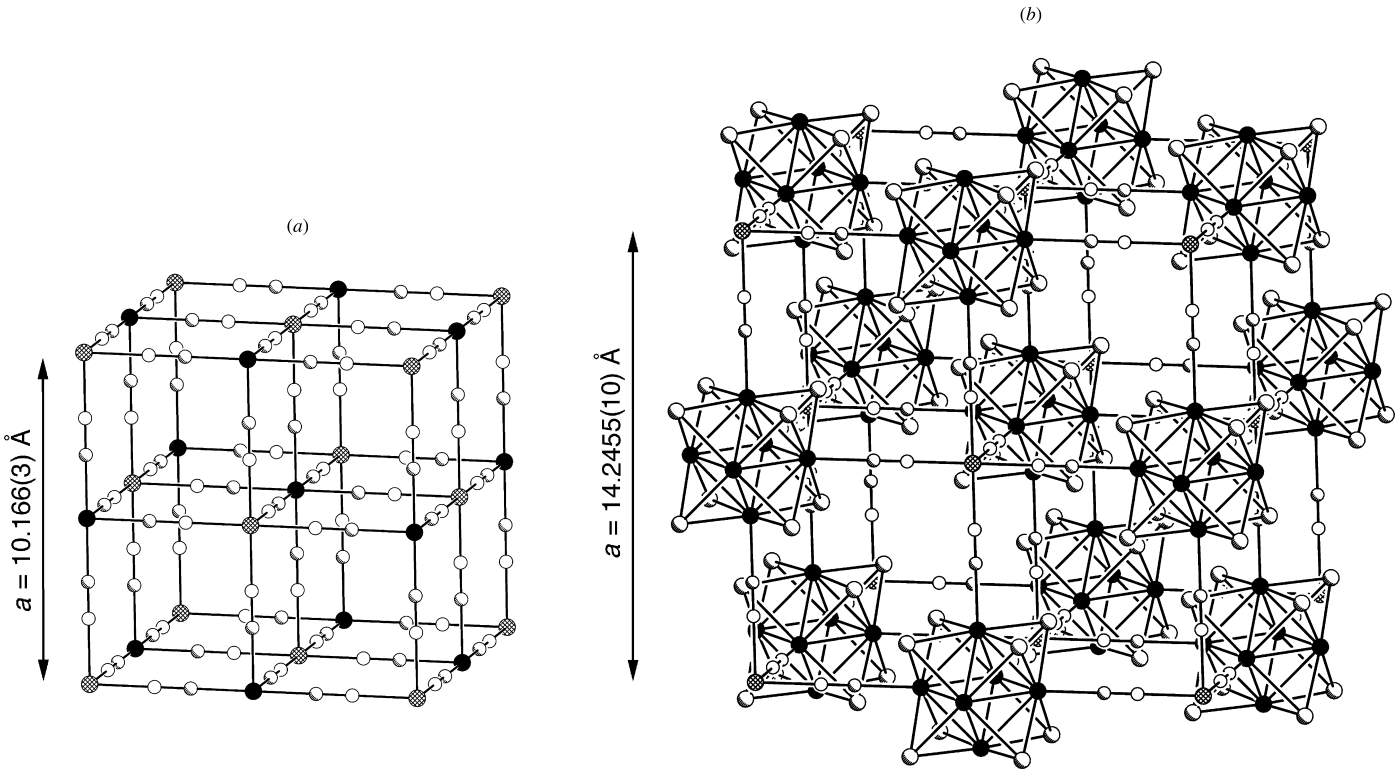

Figure 7. Unit cells of Prussian blue, $Fe_4[Fe(CN)_6]_3 \cdot 14H_2O$ (*a*), and its cluster-expanded analogue, $Fe_4[Re_6Se_8(CN)_6]_3 \cdot 36H_2O$ (*b*). Black, cross-hatched, large shaded, small shaded, and open spheres represent Fe^{2+} or Re, Fe^{3+}, Se, C, and N atoms, respectively; water molecules are ommitted for clarity. Note that only 75% of the $[Fe(CN)_6]^{4-}$ and $[Re_6Se_8(CN)_6]^{4-}$ sites within each framework are occupied, and these vacancies create even larger cavities in the framework.

cluster-expanded Prussian blue analogues have now been prepared and characterized in detail, including $Ga_4[Re_6Se_8(CN)_6]_3 \cdot 38H_2O$ and $Ni_3[Re_6Se_8(CN)_6]_2 \cdot 33H_2O$ (204, 205). Importantly, the solids can be fully dehydrated with retention of their framework structure, and nitrogen sorption isotherms confirm Type I behavior, with a significantly enhanced sorption capacity compared to the corresponding noncluster solids. Given the high concentration of coordinatively unsaturated metal sites within their frameworks, these compounds should be of some interest for study as homogeneous catalysts.

Reactions similar to reaction 5 have resulted in numerous cyano-bridged cluster-containing solids, and these are enumerated in Table V. While all but a

TABLE V
Hexanuclear Cluster–Cyanide Frameworks Prepared via Solution Assembly

Compound	Dimensionality	References
$(Me_4N)_2Mn[Nb_6Cl_{12}(CN)_6]$	3D	206
$[M(H_2O)_4]_3[W_6S_8(CN)_6] \cdot 23H_2O$ (M = Mn, Fe, Co, Zn)	3D	207
$K_2[Zn(H_2O)_2]_2[W_6S_8(CN)_6] \cdot 26H_2O$	3D	207
$[Mn(^i PrOH)_2(H_2O)]_2[Re_6S_8(CN)_6] \cdot 2^i PrOH$	3D	208
$Cs_2[trans\text{-}M(H_2O)_2][Re_6S_8(CN)_6]$ (M = Mn, Fe, Zn, Cd)	2D	180
$(Pr_4N)_2[M(H_2O)_4][Re_6S_8(CN)_6]$ (M = Mn, Ni)[a]	1D	209
$[Co_2(H_2O)_4][Re_6S_8(CN)_6] \cdot 10H_2O$[a]	3D	210
$Cs_2Co[Re_6S_8(CN)_6] \cdot 2H_2O$	2D	211
$Cs_2[Co_2(H_2O)_2][Re_6S_8(CN)_6] \cdot 2H_2O$	2D	210
$(Pr_4N)_2Co[Re_6S_8(CN)_6] \cdot 2H_2O$	1D	211
$[Cu(1,2S,2S,4\text{-butanetetramene})]_2[Re_6X_8(CN)_6] \cdot xH_2O$ (X = S, Se, Te)	2D	212
$[Zn(H_2O)]_2[Re_6S_8(CN)_6] \cdot 7H_2O$	3D	180
$[Cd_2(H_2O)_4][Re_6S_8(CN)_6] \cdot 14H_2O$	3D	205
$Cs_2[trans\text{-}M(H_2O)_2]_3[Re_6Se_8(CN)_6]_2 \cdot xH_2O$ (M = Mn, Fe, Co, Ni, Cd)	3D	180, 213
$Na[Mn(salen)]_3[Re_6Se_8(CN)_6]$[b]	3D	214
$Fe_4[Re_6Se_8(CN)_6]_3 \cdot 36H_2O$[a]	3D	204
$H[cis\text{-}M(H_2O)_2][Re_6Se_8(CN)_6]_2 \cdot 2H_2O$ (M = Fe, Co, Ni)	3D	204
$Co_3[Re_6Se_8(CN)_6]_2 \cdot 25H_2O$[a]	3D	204
$[Co(H_2O)_3]_4[Co_2(H_2O)_4][Re_6Se_8(CN)_6] \cdot 44H_2O$	3D	210
$(H_3O)_2Co_3[Re_6Se_8(CN)_6] \cdot 14.5H_2O$	3D	213
$Ni_3[Re_6Se_8(CN)_6]_2 \cdot 33H_2O$[a]	3D	204
$(H_3O)_2Zn_3[Re_6Se_8(CN)_6]_2 \cdot 20H_2O$[a]	3D	215
$Na_2Zn_3[Re_6Se_8(CN)_6]_2 \cdot 24H_2O$[a]	3D	216
$[Zn(H_2O)_6]Zn_3[Re_6Se_8(CN)_6] \cdot 18H_2O$	3D	216
$[Zn(H_2O)]_2[Re_6Se_8(CN)_6] \cdot 13H_2O$[a]	2D	216
$Ga[Re_6Se_8(CN)_6]_2 \cdot 6H_2O$[a]	3D	204
$Ga_4[Re_6Se_8(CN)_6]_3 \cdot 38H_2O$[a]	3D	203
$(H_3O)[M(dmf)_3(H_2O)_3][Re_6Se_8(CN)_6]$ (M = Nd, Pr, Ho)	3D	217
$[Mn(salen)]_4[Re_6Te_8(CN)_6]$	2D	218
$Fe_4[Re_6Te_8(CN)_6]_3 \cdot 27H_2O$[a]	3D	205

[a] This compound represents a direct expansion of a noncluster metal–cyanide framework.
[b] *N,N*-Ethylenebis(salicylideneiminato) (2−) = salen.

few of the examples are based upon octahedral Re_6 clusters, recently frameworks incorporating $[W_6S_8(CN)_6]^{6-}$ and $[Nb_6Cl_{12}(CN)_6]^{4-}$ clusters have been reported (206, 207). Furthermore, the possibility of introducing trigonal-prismatic clusters such as $[W_6CCl_{12}(CN)_6]^{3-}$ into frameworks of this type is currently under investigation (219). Note that many of the entries in Table V correspond to a direct expansion of a noncluster metal-cyanide framework. In fact, of the simple known structure types featuring octahedral $[M(CN)_6]^{n-}$ units, all but three have now been observed in an expanded form (204). A number of applications have also been demonstrated for these phases, including molecular sieving in $Ga_4[Re_6Se_8(CN)_6]_3$ (204), ion exchange in $Na_2Zn_3[Re_6Se_8(CN)_6]_2 \cdot 24H_2O$ (216), and size-selective chemical sensing in $[Co_2(H_2O)_4][Re_6S_8(CN)_6]_2 \cdot 10H_2O$ (210). As a material of potential utility in performing magnetic separations, the synthesis of a microporous magnet by incorporating paramagnetic cluster units capable of engaging in magnetic exchange interactions with the surrounding metal ions presents an interesting additional challenge (220).

Bridging ligands other than cyanide can of course be used to connect clusters into a solid framework. Thus far, this has mainly been implemented with the formation of 1D structures using site-differentiated clusters such as *cis*-$[Re_6Se_8(PPh_3)_4(4,4'\text{-bpy})_2]^{2+}$ (bpy = bipyridine) and *trans*-$[Re_6Se_8(PEt_3)_4(4,4'\text{-bpy})_2]^{2+}$ (201). As an illustrative example, reaction of [*trans*-$Re_6Se_8(PEt_3)_4(4,4'\text{-bpy})_2](SbF_6)_2$ with $Co(NO_3)_2$ in methanol–dichloromethane–ether mixture produces the solid $[Co(NO_3)_3][trans\text{-}Re_6Se_8(PPh_3)_4(4,4'\text{-bpy})_2](SbF_6)$, featuring sinusoidal chains with alternating $[Re_6Se_8]^{2+}$ cluster cores and Co^{2+} ions linked through 4,4′-bpy (176). Ultimately, continuation of this strategy could lead to the formation of highly porous 3D frameworks with adjustable components.

B. Supramolecular Assemblies

With the presence of chelating ligands on the metal ions, reactions related to those just discussed can frequently be directed toward the formation of supramolecular assemblies. Quite a number of these have now been realized that incorporate a single, central hexacyanide cluster (45, 163, 221–226). Here, a reliable strategy is to tie up all but one of the coordination sites on the metal ion, as exemplified with the reaction between $[Re_4Os_2Se_8(CN)_6]^{3-}$ and $[(Me_6tren)Cu(CF_3SO_3)]^+$ [Me_6tren = tris(2-(dimethylamino)ethyl)amine] in acetonitrile to give the cyano-bridged assembly $\{Re_4Os_2Se_8[CNCu(Me_6tren)]_6\}^{9+}$ depicted in Fig. 8 (45). This assembly is of particular interest, because it exhibits weak ferromagnetic exchange coupling ($J \sim 0.4\ cm^{-1}$) between the $S = \frac{1}{2}$ cluster core and the peripheral $S = \frac{1}{2}\ Cu^{2+}$ ions. Alternatively, one may simply use a monocyanide complex as a capping ligand, as in the synthesis of $\{Mo_6Cl_8[NCMn-$

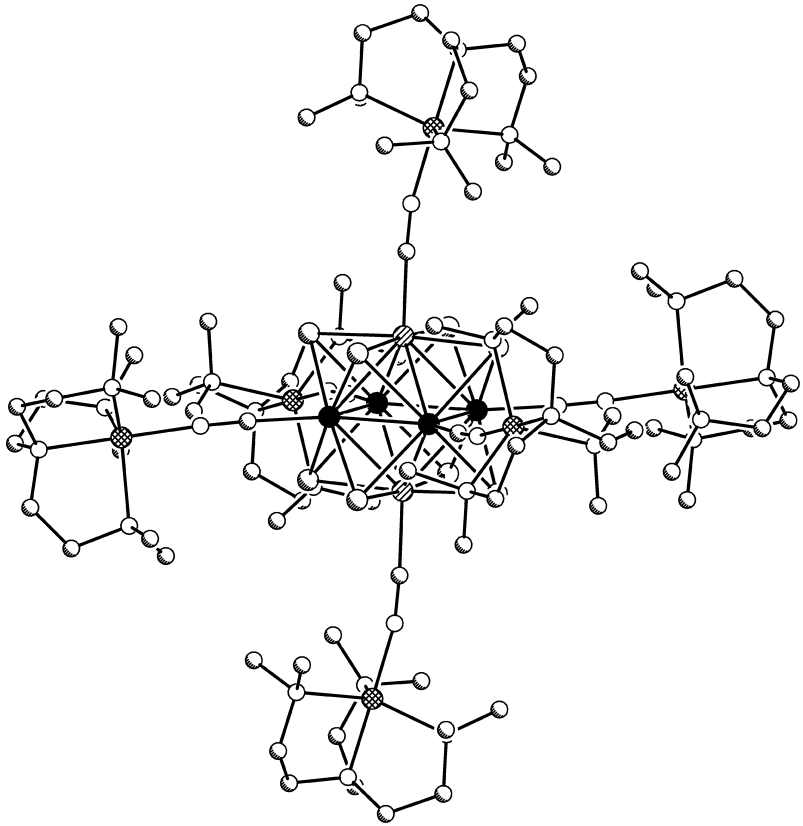

Figure 8. Structure of *trans*-$\{Re_4Os_2Se_8[CNCu(Me_6tren)]_6\}^{9+}$. Black, hatched, large shaded, cross-hatched, small shaded, and white spheres represent Re, Os, Se, Cu, C, and N atoms, respectively; H atoms have been ommitted for clarity. Note that this assembly occurs together with the cis isomer in a 2:1 ratio, and that the Re and Os sites could not actually be resolved crystallographically.

$(CO)_2Cp]_6\}^{2-}$ Cp = cyclopentadienyl through the reaction between $[Mo_6Cl_8(CF_3SO_3)_6]^{2-}$ and $[CpMn(CO)_2(CN)]^-$ in dichloromethane (163).

Site-differentiated clusters such as $[Re_6Se_8(PEt_3)_5(MeCN)]^{2+}$ and *cis*- and *trans*-$[Re_6Se_8(PEt_3)_4(MeCN)_2]^{2+}$ provide convenient building units for synthesizing a variety of multicluster assemblies. These species are readily obtained via reaction of the corresponding mono- and di-iodo cluster complexes with $AgSbF_6$ in acetonitrile (170, 171). In particular, Zheng and co-workers (201) employed a selection of pyridyl-based ligands to connect the clusters. Established examples include the dicluster $[(PEt_3)_5Re_6Se_8(\mu\text{-}4,4'\text{-bpy})Re_6Se_8(PEt_3)_5]^{4+}$ (173), the

triangular tricluster $\{[(PEt_3)_5Re_6Se_8]_3(\mu_3\text{-}L)\}^{6+}$ (L = 2,4,6-tri-4-pyridyl-1,3,5-triazine) (177), the square tetracluster $\{[(PEt_3)_4Re_6Se_8]_4(\mu\text{-}4,4'\text{-}bpy)_4\}^{8+}$ (174), and the heptacluster $\{Re_6Se_8[(\mu\text{-}L)Re_6Se_8(PEt_3)_5]_6\}^{14+}$ [L = (*E*)-1,2-bis(4-pyridyl) ethene] (175). Consistent with the nature of the frontier orbitals of the $[Re_6Se_8]^{2+}$ core (see Fig. 3), cyclic voltammetry experiments revealed no evidence for electronic communication between clusters within these assemblies. Interestingly, it is also possible to utilize building units of this type in forming multiclusters held together by bonds directly between cluster cores. For example, heating crystals containing $[Re_6Se_8(PEt_3)_5(MeCN)]^{2+}$ under dynamic vacuum results in the dicluster $[Re_{12}Se_{16}(PEt_3)_{10}]^{4+}$, wherein the two cluster cores are fused through a rhombic interaction of exactly the type found in $Re_6Se_8Cl_2$ (see Fig. 5) (170).

VI. CONCLUDING REMARKS

Our ability to manipulate the composition of a hexanuclear cluster through both solid-state and solution routes has improved steadily in recent years. The connections between composition, geometric structure, and electronic properties are gradually emerging, such that we are now in a position where clusters having specific characteristics can be targeted. Moreover, a variety of solution-based methods by which these clusters can be assembled into extended solids and supramolecular constructs are under development. Throughout much of this, a simple analogy can be drawn between the cluster complexes and octahedral or trigonal-prismatic transition metal complexes. Indeed, one can now envision these skills integrating into a new type of chemistry, wherein compounds of ever-increasing complexity are built not just from atoms, but from finely tuned cluster units.

ACKNOWLEDGMENTS

This work was supported by NSF Grant No. CHE-0111164 and DOE Grant No. DE-FG03-01ER15257. We thank ChevronTexaco for partial support of E. J. W., Mr. N. R. M. Crawford for assistance with the electronic structure calculations, and Dr. S. A. Baudron for helpful discussions.

ABBREVIATIONS

bpy	Bipyridine
Cp	Cyclopentadienyl

DFT	Density functional theory
dmf	Dimethylformamide (ligand)
DMF	Dimethylformamide (solvent)
dmso	Dimethyl sulfoxide (ligand)
DMSO	Dimethyl sulfoxide (solvent)
dpph	$Ph_2PCH_2CH_2CH_2CH_2CH_2CH_2PPh_2$
EPR	Electron paramagnetic resonance
HOMO	Highest occupied molecular orbital
LUMO	Lowest occupied molecular orbital
Me_6tren	Tris(2-(dimethylamino)ethyl)amine
NMR	Nuclear magnetic resonance
py	Pyridine (ligand)
salen	*N*,*N*′-Ethylenebis(salicylideneiminato)
THF	Tetrahydrofuran
0D	Zero dimensional
1D	One dimensional
2D	Two dimensional
3D	Three dimensional

REFERENCES

1. A. Simon, *Angew. Chem. Int. Ed. Engl.*, *27*, 159 (1988).
2. A. Perrin, C. Perrin, and M. Sergent, *J. Less-Common Met.*, *137*, 241 (1988).
3. S. C. Lee and R. H. Holm, *Angew. Chem. Int. Ed. Engl.*, *29*, 840 (1990).
4. J. Köhler, G. Svensson, and A. Simon, *Angew. Chem. Int. Ed. Engl.*, *31*, 1437 (1992).
5. J. D. Corbett, *J. Alloys Comp.*, *229*, 10 (1995).
6. T. Hughbanks, *J. Alloys Comp.*, *229*, 40 (1995).
7. C. Perrin, *J. Alloys Comp.*, *262–263*, 10 (1997).
8. N. Prokopuk and D. F. Shriver, in *Advances in Inorganic Chemistry*, A. G. Sykes Ed., Academic Press, San Diego, 1999, pp. 1–49.
9. S. Cordier, F. Gulo, and C. Perrin, *Solid State Sci.*, *7–8*, 637 (1999).
10. J. D. Corbett, *Inorg. Chem.*, *39*, 5178 (2000).
11. J. C.-P. Gabriel, K. Boubekeur, S. Uriel, and P. Batail, *Chem. Rev.*, *101*, 2037 (2001).
12. T. G. Gray, *Coord. Chem. Rev.*, *243*, 213 (2003).
13. J. R. Long, L. S. McCarty, and R. H. Holm, *J. Am. Chem. Soc.*, *118*, 4603 (1996).
14. Y. V. Mironov, J. A. Cody, T. E. Albrecht-Schmitt, and J. A. Ibers, *J. Am. Chem. Soc.*, *119*, 493 (1997).
15. T. C. Zietlow, D. Nocera, and H. B. Gray, *Inorg. Chem.*, *25*, 1351 (1986).
16. R. Chevrel, M. Sergent, and J. Prigent, *J. Solid State Chem.*, *3*, 515 (1971).
17. M. Sergent and R. Chevrel, *J. Solid State Chem.*, *3*, 433 (1973).
18. R. Chevrel, M. Sergent, and Ø. Fischer, *Mater. Res. Bull.*, *10*, 1169 (1975).

19. M. Potel, P. Gougeon, R. Chevrel, and M. Sergent, *Rev. Chim. Miner.*, *21*, 509 (1984).
20. A. Simon, H. G. von Schnering, and H. Schäfer, *Z. Anorg. Allg. Chem.*, *355*, 295 (1967).
21. H. Imoto and A. Simon, *Inorg. Chem.*, *21*, 308 (1982).
22. H., Schaefer, H.G. von Schnering, K. J. Niehues, and H. G. Nieder Vahrenholz, *J. Less-Common Met.*, *9*, 95 (1965).
23. F. W. Koknat and R. E. McCarley, *Inorg. Chem.*, *11*, 812 (1972).
24. H. M. Artelt and G. Meyer, *Z. Kristallogr.*, *206*, 306 (1993).
25. R. Siepmann, H. G. von Schnering, and H. Schäfer, *Angew. Chem. Int. Ed. Engl.*, *6*, 637 (1967).
26. Y.-Q. Zheng, E. Jonas, J. Nuss, and H. G. von Schnering, *Z. Anorg. Allg. Chem.*, *624*, 1400 (1998).
27. A. Simon, *Angew. Chem. Int. Ed. Engl.*, *20*, 1 (1981).
28. H. Womelsdorf and H.-J. Meyer, *Angew. Chem. Int. Ed. Engl.*, *33*, 1943 (1994).
29. H. Womelsdorf and H.-J. Meyer, *Z. Anorg. Allg. Chem.*, *622*, 2083 (1996).
30. E. J. Welch, N. R. M. Crawford, R. G. Bergman, and J. R. Long, *J. Am. Chem. Soc.*, *125*, 11464 (2003).
31. Y.-Q. Zheng, H. G. von Schnering, and J.-H. Chang, *Z. Anorg. Allg. Chem.*, *629*, 1256 (2003).
32. E. J. Welch, C.-L. Yu, N. R. M. Crawford, and J. R. Long, *Angew. Chem. Int. Ed.* (in press).
33. Here, we employ the connectivity notation developed by Schäfer, in which superscript "i" and "a" designate inner (core anion) and outer (terminial) ligands, respectively. For further detail, see: H. Schäfer and H.-G. von Schnering, *Z. Anorg. Allg. Chem.*, *353*, 281 (1967).
34. B. Schoenfeld, J. J. Huang, and S. C. Moss, *Acta. Crystallogr., Sect. B*, *39*, 404 (1983).
35. R. A. Wheeler and R. Hoffmann, *J. Am. Chem. Soc.*, *108*, 6605 (1986).
36. F. A. Cotton and T. E. Haas, *Inorg. Chem.*, *3*, 10 (1964).
37. F. A. Cotton, *Acc. Chem. Res.*, *2*, 240 (1969).
38. T. Hughbanks and R. Hoffmann, *J. Am. Chem. Soc.*, *105*, 1150 (1983).
39. R. G. Wooley, *Inorg. Chem.*, *24*, 3519 (1985).
40. T. Hughbanks, *Prog. Solid State Chem.*, *19*, 329 (1989).
41. R. Arratia-Pérez and L. Hernadez-Acevedo, *J. Chem. Phys*., *110*, 2529 (1999).
42. R. Arratia-Pérez and L. Hernadez-Acevedo, *J. Chem. Phys*., *111*, 168 (1999).
43. H. Honda, T. Noro, K. Tanaka, and E. Miyoshi, *J. Chem. Phys*., *114*, 10791 (2001).
44. N. R. M. Crawford and J. R. Long, *Inorg. Chem.*, *40*, 3456 (2001).
45. E. G. Tulsky, N. R. M. Crawford, S. A. Baudron, P. Batail, and J. R. Long, *J. Am. Chem. Soc.*, *125*, 15543 (2003).
46. A. Deluzet, H. Duclusaud, P. Sautet, and S. A. Borshch, *Inorg. Chem.*, *41*, 2537 (2002).
47. T. Gray, C. M. Rudzinski, E. E. Meyer, R. H. Holm, and D. G. Nocera, *J. Am. Chem. Soc.*, *125*, 4755 (2003).
48. S. A. Baudron, A. Deluzet, K. Boubekeur, and P. Batail, *Chem. Commun.*, 2124 (2002).
49. T. Saito, N. Yamamoto, T. Nagase, T. Tsuboi, K. Kobayashi, T. Yamagata, H. Imoto, and K. Unoura, *Inorg. Chem.*, *29*, 764 (1990).
50. T. C. Zietlow, M. D. Hopkins, and H. B. Gray, *J. Solid State Chem.*, *57*, 112 (1985).
51. R. A. Mackay and R. F. Schneider, *Inorg. Chem.*, *6*, 549 (1967).
52. S. Dill, M. Ströbele, and H. -J. Meyer, *Z. Anorg. Allg. Chem.*, *629*, 948 (2003).
53. H. -J. Meyer and J. D. Corbett, *Inorg. Chem.*, *30*, 363 (1991).

54. J. D. Corbett, *Inorg. Synth.*, *22*, 15 (1983).
55. J. D. Franolic, J. R. Long, J. R., and R. H. Holm, *J. Am. Chem. Soc.*, *117*, 8139 (1995).
56. R. P. Ziebarth and J. D. Corbett, *J. Solid State Chem.*, *80*, 56 (1989).
57. R. P. Ziebarth and J. D. Corbett, *J. Am. Chem. Soc.*, *107*, 4571 (1985).
58. J. D. Smith and J. D. Corbett, *J. Am. Chem. Soc.*, *108*, 1927 (1986).
59. J. D. Smith and J. D. Corbett, *J. Am. Chem. Soc.*, *107*, 5704 (1985).
60. T. Hughbanks, G. Rosenthal, and J. D. Corbett, *J. Am. Chem. Soc.*, *110*, 1511 (1988).
61. H. Schäfer, H. G. von Schnering, K. J. Niehues, and H. G. Nieder-Vahrenholz, *J. Less-Common Met.*, *9*, 95 (1965).
62. A. Simon, H.-G. von Schnering, H. Wöhrle, and H. Schäfer, *Z. Anorg. Allg. Chem.*, *339*, 155 (1965).
63. D. Bauer and H. G. von Schnering, *Z. Anorg. Allg. Chem.*, *361*, 259 (1968).
64. D. Bauer, H. G. von Schnering, and H. Schäfer, *J. Less-Common Met.*, *95*, 73 (1983).
65. H. Schäfer, H.-G. v. Schnering, J. Tillack, F. Kuhnen, H. Wöhrle, and H. Baumann, *Z. Anorg. Allg. Chem.*, *353*, 281 (1967).
66. C. Fisher, S. Fiechter, H. Tributsch, G. Reck, and B. Schultz, *Ber. Bunsen-Ges. Phys. Chem.*, *96*, 1652 (1992).
67. S. S. Yarovoi, Y. I. Mironov, Y. V. Mironov, A. V. Virovets, V. E. Fedorov, U.-H. Paek, S. C. Shin, and M.-L. Seo, *Mater. Res. Bull.*, *32*, 1271 (1997).
68. A. Perrin and M. Sergent, *Bull. Soc. Chim. Fr.*, *11–12*, 66 (1980).
69. L. Leduc, A. Perrin, and M. Sergent, *Bull. Soc. Chim. Fr.*, *11–12*, I-399 (1981).
70. L. Leduc, J. Padiou, A. Perrin, and M. Sergent, *J. Less-Common Met.*, *95*, 73 (1983).
71. N. Le Nagard, A. Perrin, M. Sergent, and C. Levy-Clement, *Mater. Res. Bull.*, *20*, 1597 (1988).
72. C. Fisher, H. Colell, and H. Tributsch, *Surf. Sci. Lett.*, *280*, L267, (1993).
73. N. L. Speziali, H. Berger, G. Leicht, R. Sanjinés, G. Chapuis, and F. Lévy, *Mater. Res. Bull.*, *23*, 1597 (1988).
74. E. G. Tulsky and J. R. Long, *Chem. Mater.*, *13*, 1149 (2001).
75. J. -C. Cretenet, *Rev. Chim. Min.*, *10*, 399 (1973).
76. J. R. Long, A. S. Williamson, and R. H. Holm, *Angew. Chem. Int. Ed. Engl.*, *34*, 226 (1995).
77. J. Zhang, R. P. Ziebarth, and J. D. Corbett, *Inorg. Chem.*, *31*, 614 (1992).
78. R. P. Ziebarth and J. D. Corbett, *J. Am. Chem. Soc.*, *110*, 1132 (1988).
79. R. P. Ziebarth and J. D. Corbett, *Inorg. Chem.*, *28*, 626 (1989).
80. A. Simon, H.-G. von Schnering, and H. Schäfer, *Z. Anorg. Allg. Chem.*, *361*, 235 (1968).
81. J. A. Parsons, A. Vongvusharintra, and F. W. Koknat, *Inorg. Nucl. Chem. Lett.*, *8*, 281 (1972).
82. A. Broll, D. Juza, and H. Schäfer, *Z. Anorg. Allg. Chem.*, *382*, 69 (1970).
83. A. Lachgar and H.-J. Meyer, *J. Solid State Chem., 110*, 15 (1994).
84. T. Duraisamy and A. Lachgar, *Acta Crystallogr., Sect. C*, *58*, I85 (2002).
85. C. Perrin, S. Cordier, S. Ihmaine, and M. Sergent, *J. Alloys Comp.*, *229*, 123 (1995).
86. T. Duraisamy, J. S. Qualls, and A. Lachgar, *J. Solid State Chem., 170*, 227 (2003).
87. S. Ihmaine, C. Perrin, and M. Sergent, *C. R. Acad. Sci. Sér. 2, 303*, 1293, (1986).
88. S. Cordier, C. Perrin, and M. Sergent, *Z. Anorg. Allg. Chem.*, *619*, 621 (1993).
89. F. Ueno and A. Simon, *Acta Crystallogr., Sect. C*, *41*, 308 (1985).
90. M. Potel, C. Perrin, A. Perrin, and M. Sergent, *Mat. Res. Bull.*, *21*, 1239 (1986).

91. C. Perrin and M. Sergent, *J. Less-Common Met.*, *123*, 117 (1986).
92. A. Peppenhorst and H. L. Keller, *Z. Anorg. Allg. Chem.*, *622*, 663 (1996).
93. C. Magliocchi, X. Xie, and T. Hughbanks, *Inorg. Chem.*, *39*, 5000 (2000).
94. Y. V. Mironov, A. V. Virovets, N. G. Naumov, V. N. Ikorskii, and V. E. Fedorov, *Chem. Eur. J.*, *6*, 1361 (2000).
95. S. Ihmaine, C. Perrin, and M. Sergent, *Croatica Chem. Acta*, *68*, 877 (1995).
96. S. Ihmaine, C. Perrin, and M. Sergent, *Eur. J. Solid State Inorg. Chem.*, *34*, 169 (1997).
97. W. Bronger, H. J. Miessen, P. Muller, and R. Neugroeschel, *J. Less-Common Met.*, *105*, 303 (1985).
98. W. Bronger, M. Kanert, M. Loevenich, and D. Schmitz, *Z. Anorg. Allg Chem.*, *619*, 2015 (1993).
99. V. P. Fedin, A. A. Virovets, and A. G. Sykes, *Inorg. Chim. Acta.*, *271*, 228 (1998).
100. Note, however, that the molecular clusters $[Nb_6I_8(NH_2R)_6]$ (R = Me, Pr), featuring a reduced 22-electron core, have been extracted into solution by direct reaction of the amines with Nb_6I_{11}: F. Stollmaier and A. Simon, *Inorg. Chem.*, *24*, 168 (1985).
101. L. Leduc, A. Perrin, and M. Sergent, *C. R. Acad. Sci. Ser. 2c*, *1*, 765 (1983).
102. A. Perrin, L. Leduc, and M. Sergent, *Eur. J. Solid State Inorg. Chem.*, *28*, 919 (1991).
103. J.-C. Pilet, F. Le Traon, A. Le Traon, C. Perrin, A. Perrin, L. Leduc, and M. Sergent, *Surf. Sci.*, *156*, 359 (1985).
104. 94. L. Leduc, A. Perrin, M. Sergent, F. Le Traon, J.-C. Pilet, and A. Le Traon, *Mater. Lett.*, *3*, 209 (1985).
105. C. Perrin and M. Sergent, *J. Chem. Res. Miniprint*, 38, (1983).
106. S. Cordier, N. G. Naumov, D. Salloum, F. Paul, and C. Perrin, *Inorg. Chem.*, *43*, 219 (2004).
107. C. B. Guilbaud, K. Boubekeur, J.-C. P. Gabriel, and P. Batail, *C. R. Acad. Sci. Ser. 2c*, *1*, 765 (1998).
108. S. Uriel, K. Boubekeur, J.-C. P. Gabriel, P. Batail, and J. Orduna, *Bull. Soc. Chim. Fr.*, *133*, 783 (1996).
109. J.-C. P. Gabriel, K. Boubekeur, and P. Batail, *Inorg. Chem.*, *32*, 2894 (1993).
110. A. Slougui, A. Perrin, and M. Sergent, *J. Solid State Chem.*, *147*, 358 (1999).
111. A. Slougui, S. Ferron, A. Perrin, and M. Sergent, *J. Clust. Sci.*, *8*, 349 (1997).
112. 92. A. Slougui, A. Perrin, and M. Sergent, *Acta Crystallogr., Sect. C*, *48*, 1917 (1992).
113. E. G. Tulsky and J. R. Long, *Inorg. Chem.*, *40*, 6990 (2001).
114. C. B. Pinheiro, N. L. Speziali, and H. Berger, *Acta. Crystallogr., Sect. C*, *53*, 1178 (1997).
115. S. S. Yarovoi, Y. I. Mironov, Y. V. Mironov, A. V. Virovets, V. E. Fedorov, U. H. Paek, S. C. Shin, and M. L. Seo, *Mater. Res. Bull.*, *32*, 1271 (1997).
116. S. Mancour, M. Patel, and P. Caillet, *J. Mol. Struct.*, *162*, 1 (1987).
117. P. Brückner, G. Peters, and W. Preetz, *Z. Anorg. Allg Chem.*, *619*, 551 (1993).
118. P. Brückner, G. Peters, and W. Preetz, *Z. Anorg. Allg Chem.*, *619*, 1920 (1993).
119. A. Perrin, M. Sergent, and Ø. Fischer, *Mater. Res. Bull.*, *13*, 259 (1978).
120. A. Perrin, R. Chevrel, M. Sergent, and Ø. Fischer, *J. Solid State Chem.*, *33*, 43 (1980).
121. W. Hönle, H. D. Flack, and K. Yvon, *J. Solid State Chem.*, *49*, 157 (1983).
122. F. J. Berry and C. D. Gibbs, *J. Chem. Soc., Dalton Trans.*, 57 (1991).
123. C. Greaves, *J. Solid State Cahem.*, *92*, 148 (1991).
124. J. Neuhausen, E. W. Flinch, and W. Tremel, *Inorg. Chem.*, *35*, 5622 (1996).

125. N. G. Naumov, K. A. Brylev, Y. V. Mironov, A. V. Virovets, D. Fenske, and V. E. Fedorov, *Polyhedron*, *23*, 599 (2003).
126. P. Brückner, G. Peters, and W. Preetz, *Z. Anorg. Allg Chem.*, *620*, 1669 (1994).
127. W. Preetz and K. Harder, *Z. Anorg. Allg Chem.*, *597*, 163 (1991).
128. J. Zhang and J. D. Corbett, *J. Less-Common Met.*, *156*, 49 (1989).
129. R. P. Ziebarth and J. D. Corbett, *J. Am. Chem. Soc.*, *111*, 3272 (1989).
130. J. Zhang, R. P. Ziebarth, and J. D. Corbett, *Inorg. Chem.*, *31*, 614 (1992).
131. R. P. Ziebarth and J. D. Corbett, *J. Less-Common Met.*, *137*, 21 (1988).
132. G. Rosenthal and J. D. Corbett, *Inorg. Chem.*, *27*, 53 (1988).
133. J. Zhang and J. D. Corbett, *Inorg. Chem.*, *30*, 431 (1991).
134. T. Hughbanks, G. Rosenthal, and J. D. Corbett, *J. Am. Chem. Soc.*, *108*, 8289 (1986).
135. R.-Y. Qi and J. D. Corbett, *Inorg. Chem.*, *33*, 5727 (1994).
136. R. D. Hogue and R. E. McCarley, *Inorg. Chem.*, *9*, 1354 (1970).
137. W. C. Dorman and R. E. McCarley, *Inorg. Chem.*, *13*, 491 (1974).
138. V. Kolesnichenko and L. Messerle, *Inorg. Chem.*, *37*, 3660 (1998).
139. D. N. T. Hay, D. C. Swenson, and L. Messerle, *Inorg. Chem.*, *41*, 4700 (2002).
140. F. A. Cotton and M. F. Curtis, *Inorg. Chem.*, *2*, 241 (1965).
141. W. M. Carmichael and D. A. Edwards, *J. Inorg. Nucl. Chem.*, *29*, 1535 (1967).
142. J. E. Fergusson, B. H. Robinson, and C. J. Wilkins, *J. Chem. Soc. A*, 486 (1967).
143. F. Stollmaier and A. Simon, *Inorg. Chem.*, *24*, 168 (1985).
144. F. Rogel and J. D. Corbett *J. Am. Chem. Soc.*, *112*, 8198 (1990).
145. C. E. Runyan and T. Hughbanks, *J. Am. Chem. Soc.*, *116*, 7909 (1994).
146. C. Magliocchi, X. Xie, and T. Hughbanks, *Inorg. Chem.*, *39*, 5000 (2000).
147. F. A. Cotton, M. Shang, and W. A. Wojtcak, *Angew. Chem. Int. Ed. Engl.*, *31*, 1050 (1992).
148. L. Chen, F. A. Cotton, and W. A. Wojtczak, *Inorg. Chem.*, *35*, 2998 (1996).
149. F. A. Cotton, L. Chen, and A. J. Schultz, *Compt. Rend.*, *323*, 539 (1996).
150. F. A. Cotton, J. Lu, M. Shang, and W. A. Wojtczak, *J. Am. Chem. Soc.*, *116*, 4364 (1994).
151. T. Saito, N. Yamamoto, T. Yamagata, and H. Imoto, *J. Am. Chem. Soc.*, *110*, 1646 (1988).
152. T. Saito, A. Yoshikawa, T. Yamagata, H. Imoto, and K. Unoura, *Inorg. Chem.*, *28*, 3588 (1989).
153. M. Emirdag-Eanes and J. A. Ibers, *Inorg. Chem.*, *41*, 6170 (2002).
154. S. J. Hilsenbeck, V. G. Young, Jr., and R. E. McCarley, *Inorg. Chem.*, *33*, 1822 (1994).
155. X. Zhang and R. E. McCarley, *Inorg. Chem.*, *34*, 2678 (1995).
156. X. Xie and R. E. McCarley, *Inorg. Chem.*, *34*, 6124 (1995).
157. M. Ebihara, K. Toriumi, and K. Saito, *Inorg. Chem.*, *27*, 13 (1988).
158. M. Ebihara, K. Toriumi, and K. Saito, *Gazz. Chim. Ital.*, *125*, 87 (1995).
159. S. Uriel, K. Boubekeur, P. Batail, and J. Orduna, *Angew. Chem. Int. Ed. Engl.*, *35*, 1544 (1996).
160. S. Uriel, K. Boubekeur, P. Batail, J. Orduna, and E. Canadell, *Inorg. Chem.*, *34*, 5307 (1995).
161. K. Jödden and H. Schäfer, *Z. Anorg. Allg. Chem.*, *430*, 5 (1977).
162. D. H. Johnston, D. C. Gaswick, M. C. Lonergan, C. L. Stern, and D. F. Shriver, *Inorg. Chem.*, *31*, 1869 (1992).
163. D. H. Johnston, C. L. Stern, and D. F. Shriver, *Inorg. Chem.*, *32*, 5170 (1993).
164. V. O. Kennedy, C. L. Stern, and D. F. Shriver, *Inorg. Chem.*, *33*, 5967 (1994).

165. N. Prokopuk, C. S. Weinert, V. O. Kennedy, D. P. Siska, H.-J. Jeon, C. L. Stern, and D. F. Shriver, *Inorg. Chim. Acta*, *300–302*, 951 (2000).
166. S. Jin, J. Adamchuk, B. Xiang, and F. J. DiSalvo, *J. Am. Chem. Soc.*, *124*, 9229 (2002).
167. T. G. Gray and R. H. Holm, *Inorg. Chem.*, *41*, 4211 (2002).
168. J. C. Sheldon, *J. Chem. Soc.*, 3106 (1960).
169. V. P. Lessmeister and H. Schäfer, *Z. Anorg. Allg Chem.*, *417*, 171 (1975).
170. Z. Zheng, J. R. Long, and R. H. Holm, *J. Am. Chem. Soc.*, *119*, 2163 (1997).
171. M. W. Willer, J. R. Long, C. C. McLauchlan, and R. H. Holm, *Inorg. Chem.*, *37*, 328 (1998).
172. Z. Zheng and R. H. Holm, *Inorg. Chem.*, *36*, 5173 (1997).
173. Z. Zheng, T. G. Gray, and R. H. Holm, *Inorg. Chem.*, *38*, 4888 (1999).
174. H. D. Selby, Z. Zheng, T. G. Gray, and R. H. Holm, *Inorg. Chim. Acta*, *312*, 205 (2001).
175. B. K. Roland, C. Carter, and Z. Zheng, *J. Am. Chem. Soc.*, *124*, 6234 (2002).
176. H. D. Selby, P. Orto, M. D. Carducci, and Z. Zheng, *Inorg. Chem.*, *41*, 6175 (2002).
177. B. K. Roland, H. D. Selby, M. D. Carducci, and Z. Zheng, *J. Am. Chem. Soc.*, *124*, 3222 (2002).
178. H. D. Selby, P. Orto, and Z. Zheng, *Polyhedron*, *22*, 2999 (2003).
179. Z.-N. Chen, T. Yoshimura, M. Abe, Y. Sasaki, S. Ishizaka, H.-B. Kim, and N. Kitamura, *Angew. Chem. Int. Ed. Engl.*, *40*, 239 (2001).
180. L. G. Beauvais, M. P. Shores, and J. R. Long, *Chem. Mater.*, *10*, 3783 (1998).
181. T. Yoshimura, Z.-N. Chen, A. Itasaka, M. Abe, Y. Sasaki, S. Ishizaka, N. Kitamura, S. S. Yarovoi, S. F. Solodovnikov, and V. E. Fedorov, *Inorg. Chem.*, *42*, 4857 (2003).
182. D. Sun and T. Hughbanks, *Inorg. Chem.*, *38*, 992 (1999).
183. X. Xie and T. Hughbanks, *Inorg. Chem.*, *41*, 4857 (2002).
184. R. Quigley, P. A. Barnard, C. L. Hussey, and K. R. Seddon, *Inorg. Chem.*, *31*, 1255 (1992).
185. C. L. Hussey, R. Quigley, and K. R. Seddon, *Inorg. Chem.*, *34*, 370 (1995).
186. N. E. Cooke, T. Kuwana, and J. Espenson, *Inorg. Chem.*, *10*, 1081 (1971).
187. P. Batail, K. Boubekeur, M. Fourmigué, A. Dolbecq, J.-C. Gabriel, A. Guirauden, C. Livage, and S. Uriel, *New J. Chem.*, *18*, 999 (1994).
188. R. D. Mussell and D. G. Nocera, *Inorg. Chem.*, *29*, 3711 (1990).
189. C. Guilbaud, A. Deluzet, B. Domercq, P. Molinié, C. Coulon, K. Boubekeur, and P. Batail, *Chem. Commun.*, 1867 (1999).
190. T. Yoshimura, S. Ishizaka, Y. Sasaki, H.-B. Kim, N. Kitamura, N. G. Naumov, M. N. Sokolov, and V. E. Fedorov, *Chem. Lett.*, 1121 (1999).
191. T. Yoshimura, K. Umakoshi, Y. Sasaki, and A. Sykes, *Inorg. Chem.*, *38*, 5557 (1999).
192. M. Ebihara, K. Isobe, Y. Sasaki, and K. Saito, *Inorg. Chem.*, *31*, 1644 (1992).
193. Interestingly, this ordering is reversed for the analogous reductions in *cis*- and *trans*-$[Re_4Os_2Se_8(PEt_3)_6]^{4+}$ (113).
194. T. Hughbanks, *Prog. Solid St. Chem.*, *19*, 329 (1989).
195. A. W. Maverick and H. B. Gray, *J. Am. Chem. Soc.*, *103*, 1298 (1981).
196. A. W. Maverick, J. S. Najdzionek, D. MacKenzie, D. Nocera, and H. B. Gray, *J. Am. Chem. Soc.*, *105*, 1878 (1983).
197. J. A. Jackson, C. Turro, M. D. Newsham, and D. Nocera, *J. Phys. Chem.*, *94*, 4500 (1990).
198. R. N. Ghosh, G.L. Baker, C. Ruud, and D.G. Nocera, *Appl. Phys. Lett.*, *75*, 2885 (1999).

199. T. G. Gray, C. M. Rudzinski, D. G. Nocera, and R. H. Holm, *Inorg. Chem.*, *38*, 5932 (1999).
200. T. Yoshimura, S. Ishizaka, K. Umakoshi, Y. Sasaki, H.-B. Kim, and N. Kitamura, *Chem. Lett.*, 697 (1999).
201. H. D. Selby, B. K. Roland, and Z. Zheng, *Acc. Chem. Res.*, *36*, 933 (2003).
202. N. G. Naumov, A. V. Virovets, and V. E. Fedorov, *J. Struct. Chem.*, *41*, 499 (2000).
203. H. J. Buser, D. Schwarzenbach, W. Petter, and A. Ludi, *Inorg. Chem.*, *16*, 2704 (1977).
204. M. V. Bennett, L. G. Beauvais, M. P. Shores, and J. R. Long, *J. Am. Chem. Soc.*, *123*, 8022 (2001).
205. M. P. Shores, L. G. Beauvais, and J. R. Long, *Inorg. Chem.*, *38*, 1648 (1999).
206. B. Yan, H. Zhou, and A. Lachgar, *Inorg. Chem.*, *42*, 8818 (2003).
207. S. Jin and F. J. DiSalvo, *Chem. Mater.*, *14*, 3448 (2002).
208. N. G. Naumov, D. V. Soldatov, J. A. Ripmeester, S. B. Artemkina, and V. E. Federov, *Chem. Commun.*, 571 (2001).
209. N. G. Naumov, S. B. Artemkina, A. V. Virovets, and V. E. Fedorov, *J. Solid State Chem.*, *153*, 195 (2000).
210. L. G. Beauvais, M. P. Shores, and J. R. Long, *J. Am. Chem. Soc.*, *122*, 2763 (2000).
211. N. G. Naumov, S. B. Artemkina, A. V. Virovets, and V. E. Fedorov, *Solid State Sci.*, *1*, 473 (1999).
212. M. P. Shores, L. G. Beauvais, and J. R. Long, *J. Am. Chem. Soc.*, *121*, 775 (1999).
213. N. G. Naumov, A. V. Virovets, M. N. Sokolov, S. B. Artemkina, and V. E. Fedorov, *Angew. Chem. Int. Ed. Engl.*, *37*, 1943 (1998).
214. Y. Kim, S.-M. Park, and S.-J. Kim, *Inorg. Chem. Commun.*, *5*, 592 (2002).
215. N. G. Naumov, A. V. Virovets, and V. E. Fedorov, *Inorg. Chem. Commun.*, *3*, 323 (2000).
216. M. V. Bennett, M. P. Shores, L. G. Beauvais, and J. R. Long, *J. Am. Chem. Soc.*, *122*, 6664 (2000).
217. S. B. Artemkina, N. G. Naumov, A. V. Virovets, S. A. Gromilov, D. Fenske, and V. E. Fedorov, *Inorg. Chem. Commun.*, *4*, 423 (2001).
218. Y. Kim, S.-M. Park, W. Nam, and S.-J. Kim, *Chem. Commun.*, 1470 (2001).
219. E. J. Welch, S. D. H. Wong, and J. R. Long (work in progress).
220. L. G. Beauvais and J. R. Long, *J. Am. Chem. Soc.*, *124*, 12096 (2002).
221. N. Prokopuk and D. F. Shriver, *Inorg. Chem.*, *36*, 5609 (1997).
222. Y. V. Mironov, V. E. Fedorov, I. Ijjaali, and J. A. Ibers, *Inorg. Chem.*, *40*, 6320 (2001).
223. Y. Kim, S. K. Choi, S.-M. Park, W. Nam, and S.-J. Kim, *Inorg. Chem. Commun.*, *5*, 612 (2002).
224. A. Itasakam, M. Abe, T. Yosimura, K. Tsuge, M. Suzuki, T. Imamura, and Y. Sasaki, *Angew. Chem. Ing. Ed. Engl.*, *41*, 463 (2002).
225. S. B. Artemkina, N. G. Naumov, A. V. Virovets, O. Oeckler, A. Aimon, S. B. Erenburg, M. V. Bausk, and V. E. Federov, *Eur. J. Inorg. Chem.*, 1198 (2002).
226. S.-M. Park, Y. Kim, and S.-J. Kim, *Eur. J. Inorg. Chem.*, 4117 (2003).